

001
002
003
004
005
006
007
008
009
010
011
012
013
014
015
016
017
018
019
020
021
022
023
024
025
026
027
028
029
030
031
032
033
034
035
036
037
038
039
040
041
042
043
044
045
046

SAVVIDRIVER: Model-based Framework for Game-based Testing of Autonomous Vehicles in Diverse Multi-agent Traffic Scenarios

Kenneth H. Chan[†], Sol Zilberman[†], Betty H.C. Cheng[†]

Department of Computer Science and Engineering, Michigan State University, 428 S Shaw Ln, East Lansing, 48824, MI, USA.

*Corresponding author(s). E-mail(s): chengb@msu.edu;
Contributing authors: chanken1@msu.edu; zilberm4@msu.edu;

[†]These authors contributed equally to this work.

Abstract

Autonomous Vehicles (AVs) must operate safely in the face of uncertainty, including those induced by human behaviors (i.e., external human drivers). Specifically, AVs must exhibit safe responses when encountering previously unseen behaviors from human drivers with different driving styles. For example, aggressive drivers may cut off other vehicles to merge into a lane, or distracted drivers may fail to respond to changing road conditions. A key challenge is how to assess the onboard AV decision-making capabilities to detect and mitigate those potentially unsafe scenarios due to one or more external human-operated vehicles. We observe that AVs and other vehicles on the roadway may share common functional objectives (e.g., to navigate to a given target destination), but otherwise may be motivated by different non-functional objectives, such as safety, minimizing transport time, minimizing fuel consumption, etc. This paper introduces a modular and composable model- and game-based testing framework to enable an AV developer to operationally assess the robustness of an AV in response to human-based uncertainty. Specifically, this work uses goal models to declaratively specify functional and non-functional objectives of vehicles (both the AV under study and those representing external human-operated vehicles) to inform the game-based testing environment that incorporates real-world traffic infrastructure data. We demonstrate the model-based capabilities of our game-based testing approach on a number of scenarios based on real-world traffic accident data involving human drivers.

047 **1 Introduction**

048
049 Increasingly, Autonomous Vehicles (AVs) are being deployed alongside human-driven
050 vehicles (i.e., mixed traffic environments [1]), where they must safely interact with
051 other road users with different behaviors, objectives, and driving styles. To ensure
052 operational correctness and prevent failures, developers must understand how AVs
053 respond to different sources of uncertainty, including the potentially unpredictable
054 behaviors of human drivers. Uncertainty arises when a system encounters an event
055 it cannot handle, often due to incomplete information (i.e., epistemic doubt [2])
056 and/or unpredictable phenomena in its operating environment (i.e., aleatoric uncer-
057 tainty [3, 4]). During design-time testing and run-time decision-making, *human-based*
058 *uncertainty* for AVs in mixed-traffic environments results from epistemic doubt about
059 other drivers’ intentions, such as motivations, behaviors, and future decisions. **How-**
060 **ever, significant safety concerns and high resource costs limit “in the field” testing**
061 **of safety-critical systems in real-world settings [5, 6], where human-based uncertainty**
062 **poses significant challenges [7, 8, 9].** Thus, there is growing interest in the use of
063 human-like driver models and simulations to test AVs in representative operating con-
064 texts, including elements that pose uncertainty, such as mixed traffic interactions [10].
065 This paper proposes a modular, goal model-based framework that harnesses the non-
066 cooperative gaming paradigm [11] to support online testing and exploration of the
067 behavior of interacting agent vehicles, including AVs and human-operated vehicles, in
068 order to assess the robustness of AVs in response to human-based uncertainty.

069 Recently, several state-of-the-art *online learning-based testing* approaches [7, 12,
070 13, 14, 15] have assessed AV responses to uncertainty posed by interactions with
071 other vehicles. *Adversarial* online learning-based testing approaches leverage knowl-
072 edge about the objectives of the AV to discover operating contexts that cause explicit
073 AV failures (e.g., collision) [12, 14]. Other online learning-based testing approaches
074 involve game-based testing, where game-theoretic formulations of traffic scenarios are
075 used to assess AV behaviors. *Cooperative* game-based testing approaches have been
076 explored to assess the ability of the AV under study to coordinate with other vehicles,
077 where traffic participants share common objectives and exhibit mutually-beneficial
078 behavior(s) [13]. However, these approaches do not reflect the state of practice AV
079 deployment, as vehicles on the road generally do not share goals nor collaborate with
080 each other (due to constraints on human and machine communications). As a means
081 to capture an AV’s environment when deployed in real-world settings, we have pre-
082 viously proposed *non-cooperative* game-based testing to explore interactions between
083 vehicles that act independently and only consider their own selfish objectives [7].
084 Specifically, these different vehicle interactions become a source of uncertainty that
085 can be used to assess the robustness of the AV under study. Reinforcement Learning
086 (RL) [16] has been used in online learning-based testing to operationally implement
087 various types of external vehicle behavior [7, 17, 18] (i.e., RL is used to approximate
088 optimal strategies for players in a traffic-based game, which can then be used as exter-
089 nal vehicle controllers whose behavior can be used to “test” the AV system under
090 study [19]). **We observe, however, that game-based testing techniques commonly rely**
091 **on trial-and-error approaches to determine game objectives (i.e., specification of an RL**
092 **reward function) and are often tightly coupled to specific traffic scenarios.** Additionally,

these techniques lack modularity and require low-level manual code changes and/or brute-force modifications to explore any changes to operational contexts, including variations on the number and types of drivers, driving strategies, road scene changes, etc. [12, 20]. As such, existing state-of-the-art game-based testing approaches lack systematic or application-level-based support for reconfiguring specifications of vehicles (e.g., speed, driving properties), roadway infrastructure (e.g., highway, merge lanes, intersections) to explore multiple operating contexts to assess AV robustness in the face of human-based uncertainty.

This work introduces SAVVIDRIVER (**S**afe **A**utonomous **V**ehicle-to-Human-**C**ontrolled **V**ehicle **I**nteractions), a modular and composable goal model-based framework for game-based testing of AVs in diverse multi-agent traffic scenarios. Several key insights are foundational to our approach. First, goal models can be used to declaratively specify and manage game-based testing of multi-agent interactions with respect to functional and non-functional objectives. Second, by refining goal models down to the level of individual requirements that can be assessed for satisfaction/satisfice-
ment in terms of utility functions [21], we can use the utility functions to specify the reward structure for an RL-based implementation of a game-based testing framework. Finally, by taking a “separation of concerns” approach [22, 23] to goal modeling, we can separate the context-dependent functional goals from context-independent non-functional goals. This strategy allows developers to *decompose* top-level goals into a library of reusable components (i.e., subtrees) corresponding to different driving styles (e.g., aggressive driving non-functional subtree). Then a developer can *compose* different combinations and structures of subtrees from the library to facilitate the rapid reconfiguration of multi-agent game-based testing with heterogeneous/homogeneous agents.

SAVVIDRIVER supports the assessment of AV robustness in response to uncertainty posed by one or more human-based agents through game-based testing, where the discovered uncertainty can then be used to improve AV robustness (e.g., revise requirements, update vehicle behaviors, etc.). Rather than explicitly modeling uncertainty, the proposed non-cooperative game theory approach organically discovers/addresses two sources of uncertainty based on their impact on the observable behavior of the AV: (1) the uncertainty posed by previously unseen external vehicle behaviors, and (2) the uncertainty posed by the unknown/unexpected responses of the AV under study when interacting with the external vehicles in various operating contexts. Consider a developer who is interested in exploring the interaction(s) between the AV under development and different types of external human driver models to discover unexpected outcomes. First, a developer defines the participating game actors (road users such as AV, human-driven vehicles, etc.) and the environmental context (e.g., merging traffic scenario) in which they interact. A developer may declaratively specify different types of human-based driving styles (e.g., aggressive, distracted, timid, etc.) based on real-world traffic data [24, 25, 26], as well as intended AV behavior(s) (e.g., safety, comfort, etc.). Next, SAVVIDRIVER uses a variation of the KAOS goal modeling language [27] to explicitly define the functional and non-functional objectives of the actors in the game. SAVVIDRIVER supports the reuse of behavior-based templates for goal model subtrees corresponding to different human-based driving styles (e.g., an ‘aggressive’

139 driving subtree can be used in different mixed-traffic scenarios). We associate utility
140 functions [28] with leaf-level goals to assess their satisfaction [29]. The utility functions
141 can be used to inform the objective function for the corresponding agent in multi-agent
142 games. As the agents for the AV and human-operated vehicles pursue their respective
143 goals while operating in the traffic scenarios under study (e.g., lane merging), unex-
144 pected and unsafe behavior may be exhibited by one or more of the agents due to
145 their unanticipated interaction(s). The discovered behavior of both AV and human-
146 operated vehicles can be used to assess and potentially improve the robustness of the
147 AV and inform changes to goal models to explore additional mixed-traffic interactions,
148 rather than editing low-level simulation code.

149 To demonstrate how SAVVIDRIVER can be used to (1) discover unexpected inter-
150 actions between AVs and external agents in the environment and (2) improve the
151 robustness of the AV with respect to human-based uncertainty, we have applied it to
152 several use cases that capture real-world traffic accident data [25, 30]. The remain-
153 der of this paper is organized as follows. Section 2 provides background information
154 and overviews enabling technologies. Section 3 describes the SAVVIDRIVER frame-
155 work, including its aggregate elements and their application to a running example.
156 Section 4 presents the results of our illustrative use cases. Section 5 discusses our
157 results. Section 6 overviews related work. Section 7 considers the threats to validity.
158 Finally, Section 8 concludes this paper and discusses future work.

159

160 2 Background

161

162 This section describes background topics and enabling technologies used in
163 SAVVIDRIVER. First, we provide an overview of existing assurance challenges for AVs
164 and simulation-based testing. Next, we discuss existing state-of-the-art approaches
165 involving game theory and RL to discover uncertainty for AVs. Finally, we describe
166 the goal modeling language and utility functions used in this work.

167

168 2.1 Challenges for Autonomous Vehicles

169

170 Advances in machine learning have improved the capabilities of AVs. Recently, a
171 number of different companies have deployed a range of AVs in real-world set-
172 tings, including Tesla’s Autopilot [31], Waymo’s Taxi services [32], and ADASTECS’s
173 autonomous bus services [33]. To avoid accidents and protect their occupants, deployed
174 AVs must demonstrate safe behavior in addition to satisfying operational constraints.
175 Based on Waymo’s 2023 safety report, AVs have the potential to reduce the frequency
176 and severity of traffic accidents in limited operating contexts [34]. However, various
177 uncertainty factors, including those introduced by machine learning and humans, have
178 been shown to cause unexpected behaviors in AVs [35]. For example, human drivers
179 exhibit a range of driving styles, including aggressive, distracted, or even malicious
180 behaviors (e.g., brake-checking, tailgating, etc.) [36]. Vehicles with these driving styles
181 have been associated with unsafe driving maneuvers on the road, such as aggressively
182 cutting off another vehicle or drifting out of a lane due to distractions [37, 38]. In
183 order to ensure AVs are capable of reacting safely when encountering these unexpected

184

maneuvers, AVs must be exposed to a wide range of human-based behaviors during training and testing [35].

2.2 Simulation-based Testing

Simulation-based testing of AVs is a type of *online testing* where the system under study is embedded and executed in a specific operating context [6]. In simulation-based testing, the operating context is represented by a virtual environment where a simulation engine manages corresponding physics, graphics, and interactions. High-fidelity simulation platforms (e.g., CARLA [39], BeamNG [40]) focus on realistic rendering and are best suited for evaluating sensor suites for AVs (e.g., computer vision models, LIDAR sensors, etc.). However, high-fidelity simulators are computationally expensive and may not scale to tasks where a large number of executions are required (e.g., RL training, search-based testing). Lightweight simulators (e.g., BARK [41], HighwayEnv [42], and our in-house simulator TINYROAD [7]) are better suited for evaluating high-level behaviors of AVs by replacing expensive realistic rendering tasks with simplified 2D models. Importantly, both types of simulation platforms implement physics engines such that vehicle actuator inputs accurately update the state of the vehicle and the operating context.

As this work focuses on discovering and evaluating high-level behavioral characteristics of vehicles, we use our in-house TinyRoad simulation platform. TinyRoad uses a standard 2D kinematic bicycle model for vehicle physics. Vehicles are represented by 2D geometry corresponding to an input vehicle type and dimensions. The roadway is represented by a graphical map of the environment, where colored lines denote roadway elements (e.g., black lines for road boundaries, yellow lines for lane boundaries, etc.). Each vehicle is associated with a controller that takes as input the state of the environment (i.e., observation o_t) and outputs a tuple for driving actions (i.e., action a_t representing throttle and steering values), at time step t . A monitoring module records the state of the environment and vehicles at each time step t , where the monitored properties are used for reward calculation and collision detection (e.g., distance between vehicle and other vehicle/road boundary within some threshold).

2.3 Game Theory for Uncertainty Exploration

In order to ensure safe behaviors, a developer may explore different techniques to test the AV before deployment. For example, a number of existing researchers have proposed the use of assurance cases and argument structures to prove the safety of AVs [43, 44, 45]. While these works provide a systematic and traceable structure to demonstrate and verify to stakeholders that the system under development is acceptably safe or satisfies some safety constraints, they do not address/propose testing techniques to discover the limitations of the system. Other existing works have explored human-based testing in a simulation environment [46, 47, 48]. However, human-based testing faces the challenges of testing bias and incurs expensive development time and effort [49]. One promising approach to model human behavior is through game theory that enables the modeling and analysis of strategic interactions between *rational decision-makers* [50]. In game theory, a game involves a number of agents that

231 interact with each other in an environment. Agents seek to achieve individual and/or
232 shared objective(s). In *cooperative* game theory, agents can collaborate to maximize
233 collective rewards [50]. However, as AVs are deployed in real-world traffic and interact
234 with traditional human-operated vehicles, it is not feasible to assume collaboration.
235 *Non-cooperative* game theory [11] better captures the relationship between road users
236 than cooperative game theory, as drivers are mainly concerned with their individ-
237 ual objectives and do not (typically) maliciously interact with other road users [7].
238 Recently, several state-of-the-art gaming approaches have used *RL* to operational-
239 ize non-cooperative games between vehicles in traffic simulations to test AVs before
240 deployment [7, 12, 14]. Chan *et al.* [7] proposed the combination of non-cooperative
241 game theory and RL to discover previously unseen or undesirable behaviors for AVs
242 in two-player games. Wachi *et al.* [14] and Hao *et al.* [12] demonstrate different ways
243 that multi-agent games and adversarial RL [51] can be used to discover failure cases
244 for rule-based vehicles in simulation. However, existing game-based testing techniques
245 largely use ad hoc and/or hard-coded techniques to generate traffic scenarios, driving
246 styles, and RL agents, where any changes (e.g., different roadways, the number/types
247 of drivers, or reward structures) may require significant low-level development effort.
248

249 **2.4 Reinforcement Learning**

250 RL is a learning-based approach, where agents learn to perform actions in an envi-
251 ronment that maximizes a reward function. Figure 1 shows a high-level overview of
252 RL, where an agent performs some action $a_t \in \mathcal{A}$ affecting the environment at each
253 timestep t . The updated state of the observable environment $o_t \in \mathcal{O}$ and the reward
254 associated with the state are then returned to the agent. The reward function informs
255 the behavior(s) of the agent, motivating it to achieve a given task. For example, an
256 agent whose objective is to complete a racing game may have a reward function that
257 motivates it to complete the race as fast as possible, stay on the track, and avoid col-
258 lisions [52]. Specifically, an agent in RL learns a *policy* $\mathcal{F}_\theta : \mathcal{E} \rightarrow \mathcal{A}$ that represents
259 a mapping between states of the environment and *optimal* actions in each of those
260 states.¹ Learning a policy involves a “trial-and-error” process, where agents make iter-
261 ative improvements to the current policy by interacting with an environment over a
262 given number of trials. During each trial (game), an agent may discover one or more
263 actions that may improve the overall reward. An optimization algorithm informs the
264 updates to the policy after each trial. Recent advances in Deep Reinforcement Learn-
265 ing (DRL) have demonstrated that Deep Neural Networks (DNNs) can be used to
266 approximate the optimal policy for a given agent [53]. DRL is often used for complex
267 tasks such as driving that may require agents to optimize high-dimensional non-linear
268 objective functions in dynamic environments [54].
269

270 In the context of RL-based behavior generation, a challenge is how to design a
271 reward function that accurately rewards and motivates a desired behavior. Existing
272 approaches often use ad-hoc development approaches to design those rewards, result-
273 ing in reward functions that are often difficult to manage or interpret and may be
274

275 ¹We use the variable \mathcal{F} to represent a policy (as opposed to the commonly used variable π in RL literature)
276 to avoid confusion with the payoff function π in game theory.

overly complex [55]. In addition, traditional approaches require “trial-and-error” low-level code changes to explore how different reward configurations result in different behaviors. In contrast, SAVVIDRIVER provides a systematic means to structure the reward function with support for updates via high-level goal model changes.

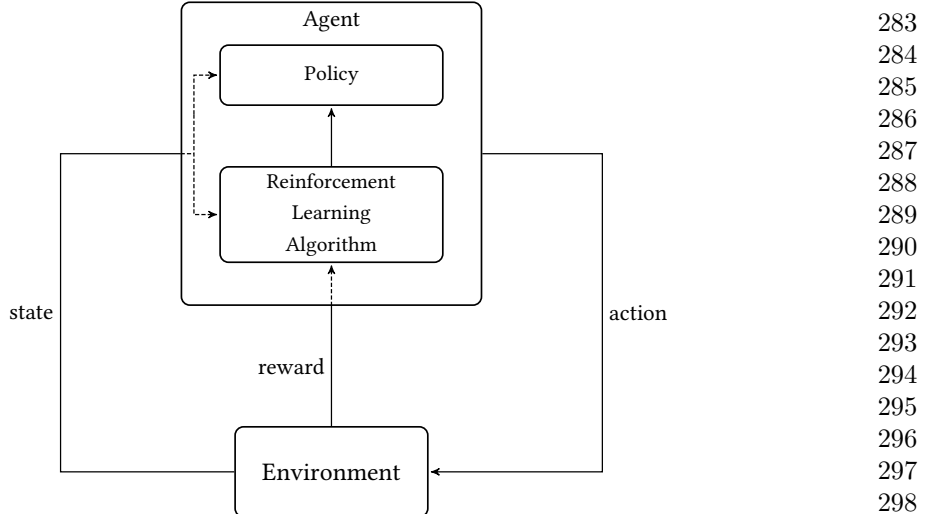


Fig. 1: A high-level overview of RL [56, 57].

2.4.1 Proximal Policy Optimization

In order to support the discovery of driving strategies that can be implemented by external vehicle controllers, SAVVIDRIVER uses the Proximal Policy Optimization (PPO) DRL technique, a well-established learning approach for control problems [16]. PPO is a first-order policy gradient method that learns the parameters θ of a stochastic policy function \mathcal{F}_θ . The goal of the PPO training is to learn a policy \mathcal{F}_θ that maximizes the probability of selecting actions that increase cumulative rewards. PPO has been shown to achieve state-of-the-art performance in continuous high-dimensional action spaces and non-stationary environments while maintaining high data-efficiency, a critical property for driving control tasks [16, 19]. Specifically, our work uses an *actor-critic-style* clipped implementation of the PPO algorithm that uses two neural networks working in tandem to approximate an optimal policy [58]. An actor-critic architecture supports stable training by combining the smooth convergence properties of policy gradient methods (actor) while reducing the variance that may result from updating parameters based on diverse training episodes (critic). For an input state o_t , the *actor* network approximates the policy $\mathcal{F}_\theta(a_t|o_t)$ (e.g., navigating to a destination using driving actions such as acceleration and braking), while the *critic* network approximates the expected reward value $V(o_t)$. An example of a reward value is the minimal time to reach the destination. Parameter updates at

323 each training step are *clipped* to the range $[1 - \epsilon, 1 + \epsilon]$ to promote better stability,
 324 where ϵ is a developer-provided hyperparameter [16]. A conservative clipping value
 325 incentivizes policy updates to stay within the developer-specified range, preventing
 326 destructive updates that may undo previously learned behavior, cause training insta-
 327 bility, or even lead to policy collapse [59]. During training, the trainable parameters
 328 θ are updated using stochastic gradient ascent to maximize an approximation of the
 329 expected cumulative reward (Expression 1 captures the objective formally),
 330

$$331 \quad L^{CLIP+VP+S}(\theta) = \hat{\mathbb{E}}[L_t^{CLIP}(\theta) - c_1 L_T^{VF}(\theta) + c_2 S[\mathcal{F}_\theta](o_t)] \quad (1)$$

332

333 where L_t^{CLIP} is the clipped surrogate objective, L^{VF} is the squared error of state val-
 334 ues, and $S[\mathcal{F}_\theta](o_t)$ is the entropy bonus [16]. The entropy bonus ensures sufficient
 335 exploration by applying perturbations to the optimization objective, encouraging more
 336 diverse actions to be selected during training [60]. Additionally, the entropy bonus
 337 has been shown to be helpful for complex tasks and may prevent early convergence
 338 to suboptimal policies [61]. Finally, PPO’s value function *VF* includes a *discount fac-*
 339 *tor* hyperparameter γ . The discount factor γ enables developers to control exploration
 340 by adjusting the proportionate weight of rewards with respect to a time horizon [16],
 341 such that earlier rewards are prioritized over later ones. A high discount factor (e.g.,
 342 0.99) encourages exploration by assigning a relatively low discount for future actions,
 343 thereby incentivizing the agent to explore states near the time horizon [62]. For exam-
 344 ple, an AV learning to merge onto a highway may find that reducing its speed to
 345 zero until the end of an episode allows it to avoid penalties from future collisions.
 346 However, this behavior prevents the successful completion of the objective (i.e., navi-
 347 gating to a destination) and is therefore suboptimal. By applying perturbations to the
 348 reward signal, the vehicle has a greater chance of exiting the suboptimal stable state
 349 by attempting new behaviors (e.g., merge maneuver).
 350

351 2.5 Goal-Oriented Requirements Engineering

352

353 Van Lamsweerde *et al.* introduced KAOS, a goal-oriented approach to requirements
 354 engineering, where a high-level goal or objective is decomposed into subgoals. Each
 355 subgoal is then recursively decomposed until a low-level leaf goal is reached [27]. At
 356 the leaf level, KAOS goals are considered requirements that are discharged to *system*
 357 *components* for satisfaction or satisficement (i.e., degree of satisfaction) [27].² While
 358 KAOS does not distinguish functional and non-functional goals explicitly, subgoal
 359 decomposition strategies can be used to specify functional goals that reflect non-
 360 functional properties. Effectively, our KAOS goal model captures the non-functional
 361 properties of driving styles in terms of the functional goals/subgoals. For example, the
 362 non-functional subgoal, ‘drive safely’, can be refined down to requirements: ‘driving
 363 at the speed limit’ and ‘maintaining a minimal trailing distance’. Those require-
 364 ments can then be handled by the system components ‘speed controller’ and ‘radar’,
 365 respectively.

366

367 ²We use the term “system components” instead of “agents” in the KAOS goal model to avoid confusion
 368 with the use of the term “agent” for AV and non-ego vehicles.

2.6 Utility Functions	369
Utility functions can be used to map system and environmental attributes to quantitative values that establish a degree of system goal satisfaction [29, 63, 64, 65]. Expression (2) shows the general structure of a utility function, where u represents a scalar utility value between $[0, 1]$, and v represents a measured property obtained from the system and its environment (e.g., vehicle speed, distance to target destination) [29].	370
	371
	372
	373
	374
	375
	376
	377

Previously, it has been shown that *utility functions* can be used to annotate KAOS leaf-level goals to measure their satisficement [29, 64, 66]. Specifically, leaf-level goals are annotated with utility functions that specify how the corresponding system component can be used to measure a quantifiable attribute of the leaf-level goal. For example, the requirement ‘driving at the speed limit’ can be quantified by the utility function shown in Expression (3), where s corresponds to the speed limit and v corresponds to the agent’s current velocity. The maximum value (i.e., *utility*) occurs when the agent is driving exactly at the speed limit (i.e., $s - v = 0$).

$$f(x) = \begin{cases} 0 & \text{if } v < .95s, v > 1.05s \\ |\frac{s-v}{0.05s}| & \text{if } .95s \leq v \leq 1.05s \end{cases} \quad (3)$$

3 Methodology

This section describes the SAVVIDRIVER framework, including details of its modeling and analysis processes. Table 1 provides a high-level glossary of the terms and their definitions used in this work. Figure 2 shows an overview of the SAVVIDRIVER framework, where circles depict processes, parallel lines depict persistent data stores, labeled arrows depict data flow between entities, and rectangles depict external entities. The SAVVIDRIVER framework takes as input real-world traffic data and the EGO under study. First, SAVVIDRIVER facilitates the development of goal models for agent objectives that reflect real-world driver behaviors. Next, SAVVIDRIVER configures the reward functions and simulated traffic scenario corresponding to the goal models. Then SAVVIDRIVER’s game-based testing process automatically trains RL-based Non-ego Vehicle (NEV) controllers that exhibit behaviors specified by their respective goal models, where NEV behaviors pose a source of uncertainty for the input EGO under study. Finally, SAVVIDRIVER supports the assessment of EGO robustness with respect to the discovered human-based uncertainty exhibited by RL-based NEV agents, which can be used to improve EGO robustness. We next describe the elements of SAVVIDRIVER in detail.

Data

Historical data, documentation, and domain expert input regarding driving data and traffic accidents are all used by the developer to identify and specify different types of driver intentions. For example, we use data collected by key federal US-based agencies

415 to identify driver behaviors that frequently resulted in undesirable traffic outcomes
416 (e.g., United States National Highway Traffic Safety Administration (NHTSA) [24,
417 25, 67], United States Department of Transportation [26], AAA Foundation for Traf-
418 fic Safety [68, 69]). These agencies are responsible for investigating traffic incidents
419 and publishing data reports that include the types of maneuvers leading up to acci-
420 dents, the statistics about characteristics and frequencies of accidents, and the details
421 for the road environments where the accidents occurred. Developers and/or domain
422 experts may use the traffic data to identify common high-level driver behaviors to fur-
423 ther explore with SAVVIDRIVER at design-time. As such, SAVVIDRIVER can be used
424 to explore human-based uncertainty found in real-world traffic scenarios [24, 25, 26],
425 as well as other possible detrimental scenarios. SAVVIDRIVER generates RL driving
426 models that are informed by real-world high-level human behavior characteristics that
427 have been documented as contributing factors to traffic accidents [24, 25, 26], often
428 due to the unpredictability/lack of knowledge about the driver intentions/maneu-
429 vers (e.g., an aggressive driver may quickly decide to cut off a vehicle without any
430 indication or safety precautions). Specifically, SAVVIDRIVER automatically explores
431 manifestations of human-based uncertainty by executing the RL driving models in
432 simulation and analyzing their dynamic interactions with the EGO under study to
433 uncover uncertainty posed by unexpected NEV maneuvers and corresponding unde-
434 sirable EGO responses. Those unexpected maneuvers/interactions constitute a form of
435 *epistemic uncertainty* as an EGO may not be able to predict and handle interactions
436 with the drivers exhibiting those maneuvers.

437 During pre-processing, domain experts identify through manual or automated
438 techniques (e.g., accident analysis procedures [26]) three key types of information, in
439 addition to the AV software under study:

- 440
- 441 • **Scenario Definition:** Concrete parameters of the identified traffic scenario that
442 describe the structural attributes (e.g., lane geometry, topography, etc.), regula-
443 tory attributes (e.g., speed limit, direction of the lane) of the traffic infrastructure,
444 and the participating vehicles (e.g., type, initial position, orientation, and velocity
445 of each vehicle).
 - 446 • **Scenario Objective:** The functional objective of each agent participating in a
447 given scenario, as identified by domain experts. For a given scenario, each agent's
448 scenario objective may capture scenario-specific maneuvers an agent should per-
449 form (e.g., merge into right lane), with respect to their initial state in the traffic
450 infrastructure.
 - 451 • **Driver Types:** The driving style (e.g., aggressive, cautious, etc.) and observed
452 behaviors (e.g., speeding, swerving, etc.) of each agent.
 - 453 • **Black-box Ego Configuration:** The AV software under study that maps envi-
454 ronment inputs to actions. For example, the AV configuration can specify a
455 traditional software-based ADAS system, an RL-based driving model, or any
456 other simulated AV software system.

457

458 Running Example: We illustrate the SAVVIDRIVER framework using a running
459 example of a merge scenario, motivated by NHTSA's 2022 accident reports [24, 70] that
460

Table 1: Overview of the terminologies used in this paper.

Term	Definition	
ITS	An Intelligent Transportation System (ITS) comprising one or more intelligent vehicle(s) (e.g., AVs) as well as one or more human-operated vehicle(s).	461 462 463 464 465 466 467 468 469
Agent	Entity with a concrete role (e.g., vehicle) that has goals and is of interest in the ITS under study. [†]	470 471 472 473 474 475 476 477 478 479 480 481 482 483 484 485
AV	An autonomous vehicle whose behavior is optimized by one or more machine learning component(s).	486 487 488 489 490
Ego	The autonomous vehicle under study.	491 492 493 494 495 496 497 498 499 500 501 502 503 504 505 506
NEV	Human-operated vehicle that is part of the operational context for the AV in the ITS.	
Functional goal	Goals that describe functions that the system should perform (e.g., arrive at destination).	
Non-functional goal	Goals that describe desired properties (e.g., defensive driving) of how a system satisfies its functional goals.	
Scenario Definition	Concrete parameters of the identified traffic scenario, including infrastructure data and initial agent states.	
Scenario Objective	The individual functional objectives of each agent in a given scenario.	
Driver Type	The driving style (e.g., aggressive, cautious, etc.) and observed behaviors (e.g., speeding, swerving, etc.) of each agent.	

[†] The term *agent* is common to the disparate techniques used in this work (e.g., goal modeling, reinforcement learning, game theory). We use the definition presented in this table whenever the term *agent* is used.

list lane merging as a frequent cause of accidents. Figure 3 provides a 2D illustration of the Intelligent Transportation System (ITS) under study. The scenario under study is a two-lane road that converges into a single lane. The participating agents include the blue EGO (the default AV under study) driving in the right lane and an orange aggressive NEV that must merge into the EGO’s lane. During game-based testing, both vehicles are instantiated in a simulated traffic scenario. During each timestep of the simulation, each vehicle takes as input the current state of the environment and uses its respective controller to perform a driving action. The blue EGO uses the default AV software under study to take actions, while the orange NEV uses the SAVVIDRIVER-generated RL-based policy to take actions, thereby exhibiting behaviors that may exploit safety properties of the default blue EGO. Therefore, each game-based testing scenario comprises the SAVVIDRIVER-trained NEV controller, a corresponding traffic scenario, and the blue EGO software under study. We view uncertainty from the perspective of an AV developer. In our running example, the blue EGO may be uncertain about the intentions and future behaviors that may be exhibited by the orange NEV as

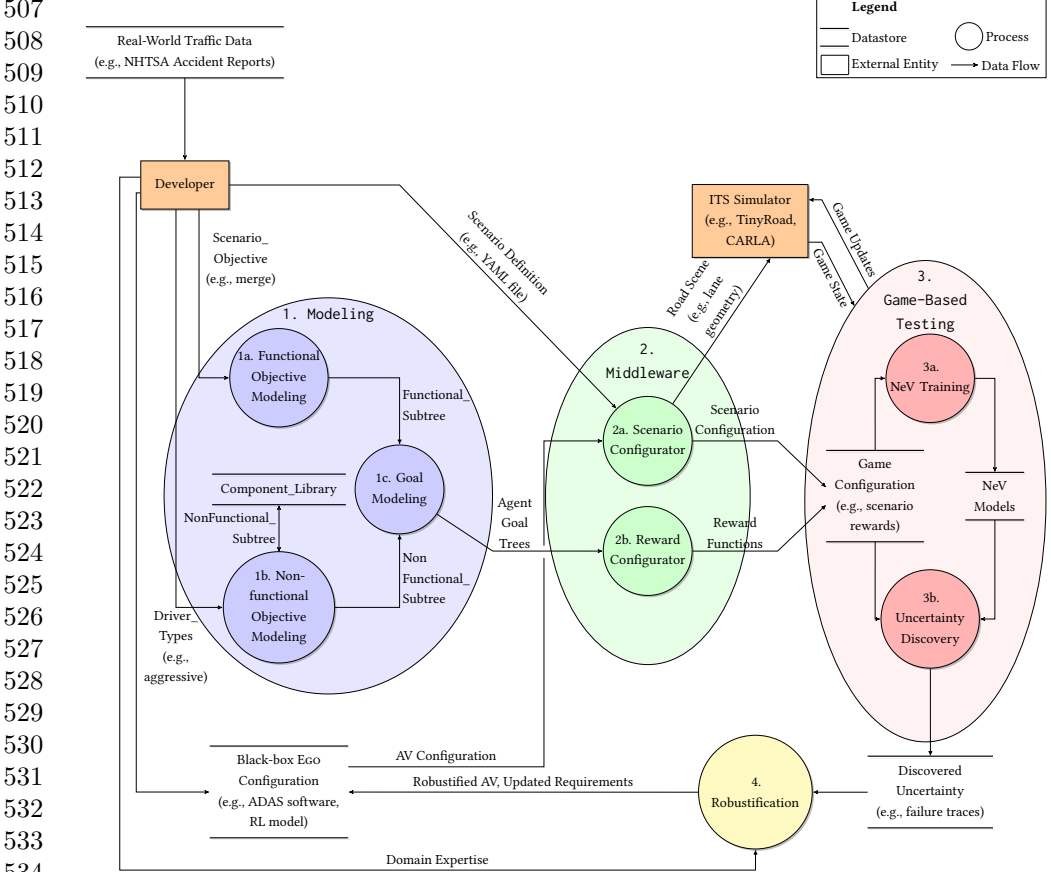


Fig. 2: Overview of SAVVIDRIVER. Purple processes represent manual modeling steps done by a Developer. Green processes represent an automated middleware compilation of Developer information. Red processes represent game-based testing components. Finally, the yellow process represents the AV robustification step of the framework, which can incorporate domain knowledge from the Developer.

the orange NEV pursues its selfish human-based objectives. Subsequently, the developer may be uncertain about how the blue EGO may respond to unexpected behaviors exhibited by the orange NEV. To this end, the objective of SAVVIDRIVER is to reduce the epistemic uncertainty that is associated with unexpected behaviors of the orange NEV by generating those behaviors during the testing phase, as a means to assess the blue EGO's responses in the presence of those behaviors, and then robustifying the blue EGO to the discovered uncertainty.

3.1 Step 1. Modeling

This step describes how agents are modeled by the **Developer** in SAVVIDRIVER; this process is used to individually develop respective goal models to describe EGO and NEV(s) behaviors. Modeling Process 1 overviews the **Developer**'s process for goal modeling promoted by SAVVIDRIVER. We use a variation of the KAOS goal modeling language to elaborate the top-level functional objective of each agent (e.g., ‘arrive at destination’). A **Developer** uses KAOS to create an AND/OR goal model to declaratively specify at a high-level *what* an agent’s objectives are and the driving style (i.e., non-functional requirements) they should exhibit when satisfying those objectives. We next describe the elements of the goal model-based decomposition strategy, which is used to model both the behavior of the EGO and NEV(s).

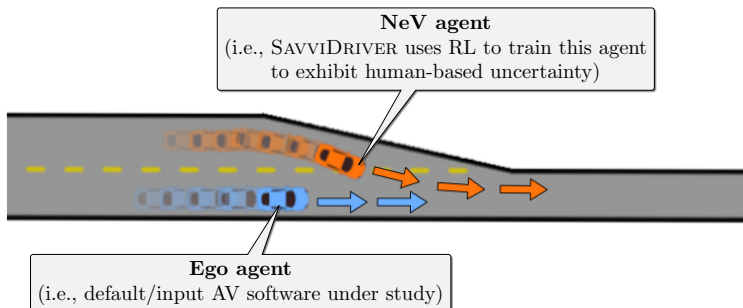


Fig. 3: Merge scenario sample showing the EGO (blue) and NEV (orange) in the TINYROADS simulator [7].

For each agent, the **Developer** refines and decomposes the agent’s top-level objective into two distinct types of subtrees: functional subtrees and non-functional subtrees. Figure 4 shows an abstract overview of goal decomposition in SAVVIDRIVER, where the top-level goal is shown in orange, *KAOS Goals* are depicted by parallelograms, and goal decomposition is represented by refinement arrows. The blue subtree in Figure 4 shows **Step 1a** of SAVVIDRIVER, where the **Developer** defines the *context-dependent functional objectives* that correspond to a *Scenario_Objective*. For example, a vehicle may have a *Scenario_Objective* of merging into the right lane of the roadway if its initial position is in a merging lane (see orange vehicle, Figure 3). The green subtree in Figure 4 shows **Step 1b** of SAVVIDRIVER, where the **Developer** defines the *context-independent non-functional objectives* corresponding to a *Driver_Type* that captures the driving style(s) a vehicle may exhibit while completing its functional objectives. For example, a vehicle may exhibit aggressive or distracted driving styles while attempting to merge into the right lane of the roadway. Finally, in **Step 1c**, the **Developer** composes the two subtrees from **Step 1a** and **Step 1b** to form the overall KAOS goal tree for the agent.

SAVVIDRIVER’s goal modeling approach facilitates and promotes modularity and reusability of agent objectives. Specifically, high-level agent objects can be decomposed into a library of reusable *components* corresponding to different driving styles,

553
554
555
556
557
558
559
560
561
562
563
564
565
566
567
568
569
570
571
572
573
574
575
576
577
578
579
580
581
582
583
584
585
586
587
588
589
590
591
592
593
594
595
596
597
598

599 represented by context-independent subtrees. Figure 5 shows how those components
 600 can be reused and composed to explore different mixed-traffic scenarios. The first row
 601 (I.) shows the merge scenario with subtree F_1 and its children $F_{1.1}$ and $F_{1.2}$ with two
 602 different non-functional subtree decompositions: aggressive and distracted. The sec-
 603 ond row (II.) shows the extraction of the non-functional subtree of each merge scenario
 604 and their addition to the Component Library. The third row (III.) shows that the sub-
 605 trees from the Component Library can be reused in a different scenario (i.e., left-turn).
 606 As such, SAVViDRIVER supports the interchange and reuse of subtrees and scenarios
 607 to discover uncertainty (e.g., unexpected interactions between an EGO and different
 608 combinations of NEVs in diverse mixed-traffic scenarios).

609

610 **Modeling Process: 1 Step 1 of SAVViDRIVER (performed by developer).**

```

611 1: /* Step 1a. Functional Objective Modeling */
612 2: > Decompose Scenario.Objective down to requirements to define Functional.Subtree.
613 3: > Annotate leaf-level requirements with utility functions.
614 4:
615 5: /* Step 1b. Non-functional Objective Modeling */
616 6: > If Driver_Type exists in Component_Library.
617 7:   > Retrieve NonFunctional_Subtree from existing Component_Library.
618 8: > Else
619 9:   > Decompose Driver_Type down to requirements to define NonFunctional.Subtree.
620 10:  > Annotate leaf-level requirements with utility functions.
621 11:  > Add NonFunctional.Subtree to Component_Library.
622 12:
623 13: /* Step 1c. Goal Modeling */
624 14: > AND-compose Functional.Subtree and NonFunctional.Subtree and attach to top-level goal.
625 15: > Return agent goal model.

```

622

623

624

625

626

627

628

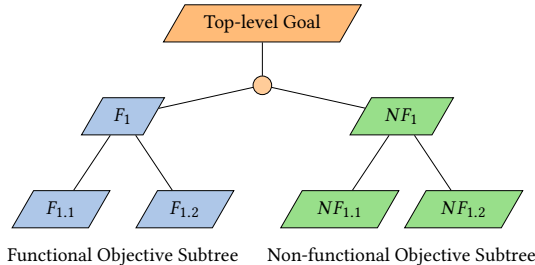
629

630

631

632

633



634 **Fig. 4:** Abstract representation of the KAOS goal tree for a vehicle in a scenario. The
 635 functional subtree decomposition is shown in blue, while the non-functional subtree
 636 decomposition is shown in green.

637

638

639

640 Consider the running example in Figure 3 involving the merge lane. We create
 641 goal models comprising their respective objectives for both the EGO and the NEV
 642 following the process described in **Step 1. Modeling**. Figure 6a and Figure 6b show
 643 sample KAOS goal models for the EGO and AGGRESSIVE-NEV, respectively. *KAOS*
 644 *Goals* are depicted by parallelograms. Goal decomposition is represented by refinement

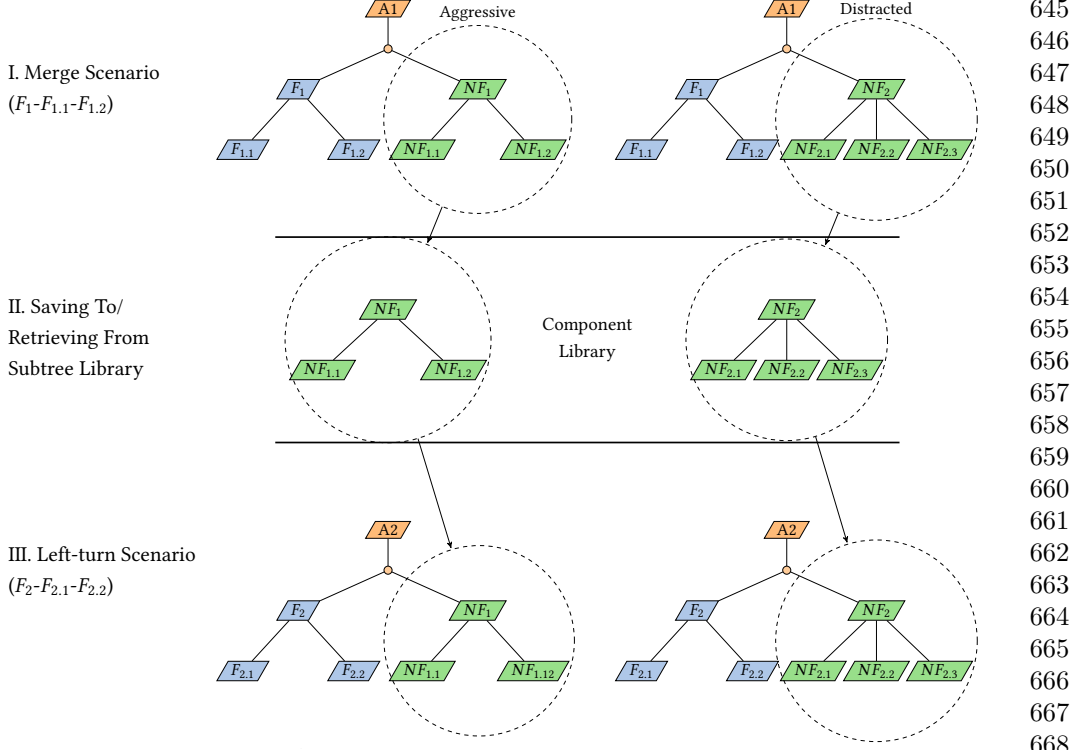
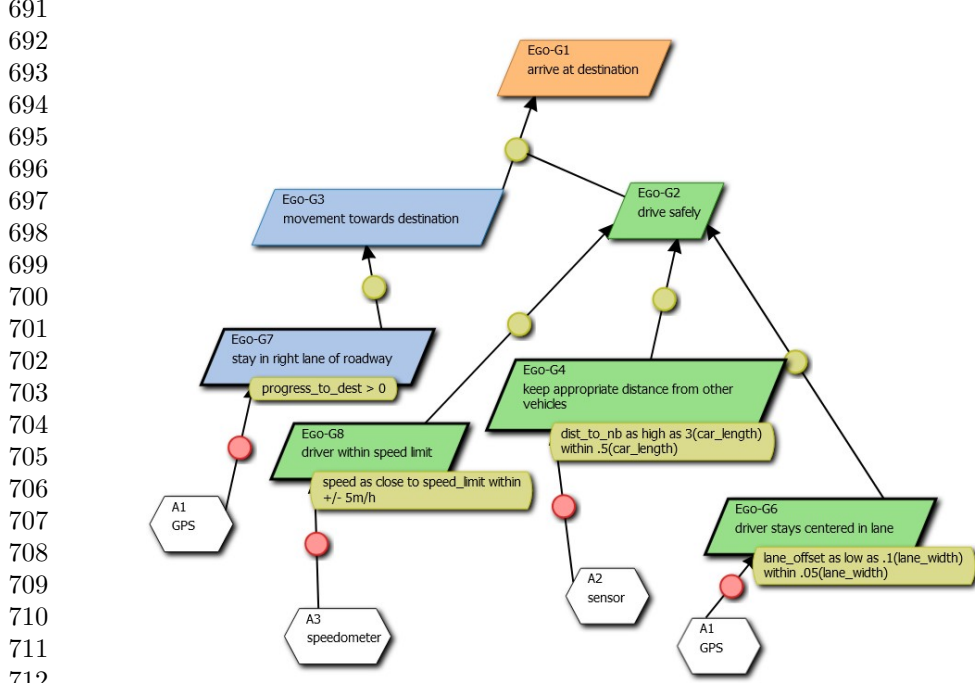


Fig. 5: Example of how modular subtrees can be reused in SAVVIDRIVER. The first row (I.) shows the merge scenario with two different non-functional objectives (i.e., aggressive ($NF_1 - NF_{1.1} - NF_{1.2}$) and distracted ($NF_2 - NF_{2.1} - NF_{2.2} - NF_{2.3}$)). The second row (II.) shows the extraction of the subtrees from the merge scenario to the **Component Library**. Finally, the third row (III.) shows the left-turn scenario, reusing the non-functional objectives from the merge scenario with a new functional objective.

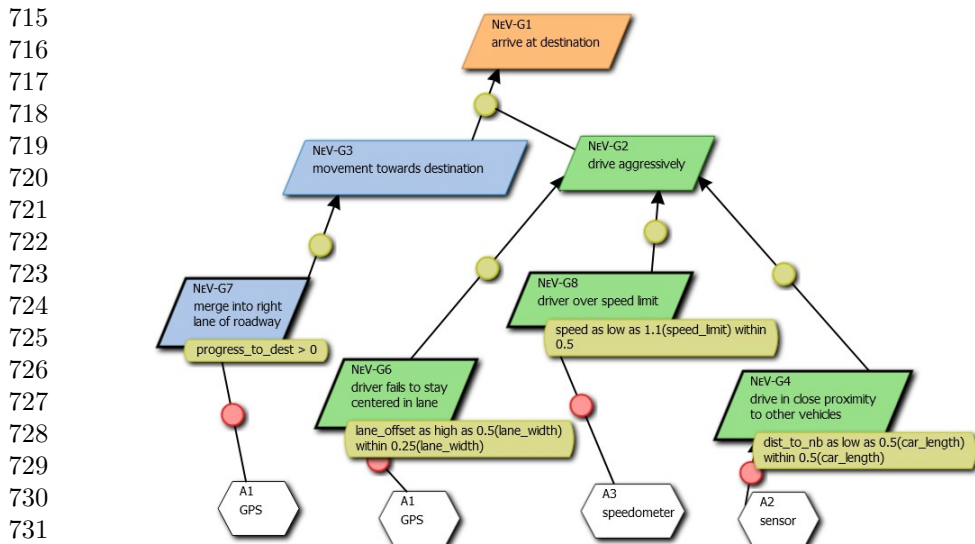
arrows. The **Developer** also specifies utility functions to be associated with leaf-level goals (represented by yellow ellipses), which are also used to specify objective functions for the driver model for each agent [29]. Blue parallelograms denote functional goals, while green parallelograms denote non-functional goals. The utility functions are discharged to system components, represented by white hexagons. We next describe the development of models for each agent in our running example in turn.

KAOS Goal Model for the AV (Figure 6a)

For the EGO, the top level goal EGO-G1 ‘arrive at destination’ is AND- decomposed into the context-dependent functional goal EGO-G2 ‘move towards destination’ (**Step 1a**) and context-independent non-functional goal EGO-G3 ‘drive safely’ (**Step 1b**). The functional goal EGO-G2 is decomposed into ITS-specific goal EGO-G7 ‘stay in right lane of roadway’. The safety goal EGO-G3 is further decomposed into subgoals. Associated with each leaf-level goal (i.e., requirement) is a utility function



(a) KAOS goal model for the EGO.



(b) KAOS goal model for AGGRESSIVE-NEV.

733
734
735
736

Fig. 6: Overview of KAOS goal models for the EGO and the AGGRESSIVE-NEV.

that quantifies its satisfaction (i.e., degree of satisfaction [27]). For example, the non-functional goal EGO-G4 ‘keep appropriate distance from other vehicles’ is formally captured by the utility function in Expression (4), where the EGO vehicle seeks to keep its current distance (`dist_to_nb`) as high as 3 car lengths. The EGO vehicle is additionally rewarded if it exceeds the minimum of 3 car lengths, with a max reward at 3.5 car lengths. Finally, **Step 1c** composes subtrees rooted at goal EGO-G2 and goal EGO-G3 via KAOS AND- relation and adds them as children to the top-level goal EGO-G1.

$$f(\text{dist_to_nb}) = \begin{cases} 0 & \text{if } \text{dist_to_nb} \leq 3 \cdot \text{car_length} \\ 1 & \text{if } \text{dist_to_nb} \geq 3.5 \cdot \text{car_length} \\ \frac{\text{dist_to_nb} - 3.0 \cdot \text{car_length}}{0.5 \cdot \text{car_length}} & \text{if } 3 \cdot \text{car_length} \leq \text{dist_to_nb} \leq 3.5 \cdot \text{car_length} \end{cases} \quad (4)$$

KAOS Goal Model for Aggressive NeV (Figure 6b)

For the AGGRESSIVE-NEV, the top level goal NEV-G1 ‘arrive at destination’ is AND-decomposed into the context-dependent functional goal NEV-G4 ‘move towards destination’ (**Step 1a**) and context-independent non-functional goal NEV-G2 ‘get to destination quickly’ (**Step 1b**). The functional goal NEV-G4 is next decomposed into ITS-specific goal NEV-G7 ‘merge into right lane of roadway’. The agent-specific goal NEV-G2 is then refined into a lower-level agent-specific goal NEV-G3 ‘drive aggressively’. The aggressive driving goal NEV-G3 is further OR-decomposed into quantified subgoals including speeding, swerving, and distance to vehicles. Finally, **Step 1c** composes subtrees rooted at goal NEV-G4 and goal NEV-G2 via KAOS AND- relation and adds them as children to the top-level goal NEV-G1 ‘arrive at destination’.

3.2 Step 2. Middleware

This section overviews how SAVVIDRIVER’s **Middleware** collates and processes information from the agent goal models and scenario specifications to coordinate the game-based testing of AVs. Specifically, the **Middleware** uses two different configurators, a **Scenario Configurator** (**Step 2a**) and a **Reward Configurator** (**Step 2b**), to automatically realize mixed-traffic interactions as a *game* between an EGO and one or more NEV(s), where driver behaviors are informed by agent-specific goal models. We next describe each configurator in turn.

2a. Scenario Configurator

We use game theory to provide the structure of the mixed-traffic scenario to support requirements-based exploration of human-based uncertainty. In our framework, a traffic scenario is captured as a game that comprises the following components: (1) the vehicles (i.e., players) of the game, (2) the actions available to each vehicle (e.g., steering, throttle), (3) the information structure (i.e., what a driver knows at a given step of the game), and (4) the objective function each driver seeks to maximize.

To this end, we formally define the mixed-traffic scenario as a non-zero-sum, non-cooperative game [11]. We view traffic scenarios as non-zero-sum games as we do not

783 enforce any constraints on the sum of player payoff functions. In contrast, in zero-
784 sum games, a player’s advantage necessarily results in an equivalent loss for the other
785 player(s) (e.g., when a player takes a bigger slice of the pie, the other players have
786 less pie available to consume). A zero-sum game is a special case of a non-zero-sum
787 game, where the total payoff is equal to zero [11, 50]. Let player set \mathcal{I} represent N
788 interacting players, where each player $p_i, p_i \in \mathcal{I}$ corresponds to a vehicle in the game
789 (see Expression (5)).

790

791

792
$$\mathcal{I} = \{p_1, p_2, \dots, p_N\}. \quad (5)$$

793

794 The gaming setup captures the number and type of agents, including the EGO
795 and one or more NEVs, as well as the operating context in which they interact,
796 such as a highway merge scenario or left-turn scenario. An **ITS Simulator** provides
797 an environment that enables games to be executed to discover uncertainty. The
798 **Scenario Configurator (Step 2a)** takes as input a **Scenario Definition** file to ini-
799 tialize the **ITS Simulator** and provide the **Scenario Configuration** as the operating
800 context for the **Game Configuration**. A sample **Scenario Definition** file is shown in
801 Listing 1. This information captures the road layout, the number and types of agents
802 in play, and their initial states (e.g., position, velocity).

803

804 **2b. Reward Configurator**

805

806 We next describe the automatic generation of each player’s reward. The KAOS model
807 serves as the “middleware” between the gaming setup and the ITS simulation, enabling
808 developers to formally realize high-level developer input in terms of low-level functional
809 goals instead of directly editing simulation code. In SAVVIDRIVER, non-cooperative
810 game theory is used to support simulation-based testing to discover previously unseen
811 traffic interactions between the EGO and one or more NEV(s). RL is used to realize
812 the non-cooperative games, where gaming interactions are captured via RL reward
813 functions. However, designing reward functions is challenging, especially for complex
814 tasks with multiple competing objectives such as mixed-traffic scenarios [71]. More-
815 over, RL-based techniques often rely on ad-hoc development approaches that result in
816 fragile/unstable reward functions; it may be unclear how modifying the reward func-
817 tion impacts observable agent behavior [55]. To this end, the **Reward Configurator**
818 (**Step 2b**) “compiles” high-level agent objectives defined in goal models into RL
819 reward functions, thereby bridging the gap between the previous modeling step and the
820 non-cooperative ITS game, to discover uncertain behaviors for a given traffic scenario.

821

822 Listing 1: Sample **Scenario Definition** file for the merge scenario.

823

824

825

826

827

828

1	map :	829
2	filename: merge_road	830
3	vehicles:	831
4	- name: Safety-Ego	832
5	position: [427, 750]	833
6	velocity: 40	834
7	- name: Aggressive-NeV	835
8	position: [370, 750]	836
9	velocity: 40	837

Recall that a scenario comprises a set of players p_i with corresponding KAOS goal models k_i . A strategy space \mathcal{S}_i represents potential strategies s_i that player i can use for decision-making [72, 73]. In RL, a strategy s_i may be represented by a DNN that maps the current state of the operating environment observed by player p_i (e.g., vehicle locations, velocities, trajectories, etc.) to an action (e.g., actuator inputs such as braking, steering, etc.). Each player p_i seeks to find the “best” strategy s_i^* based on an individual reward (payoff) function π_i . Each player’s DNN can be trained via RL to approximate the best strategy s_i^* [7, 16], which is formally specified in Expression (6):

$$s_i^* = \underset{s_i \in \mathcal{S}_i}{\operatorname{argmax}} \pi_i(s_i, s_{-i}^*), \forall s_i \in \mathcal{S}_i, \forall i \in \{1, \dots, N\}, \quad (6)$$

where s_{-i}^* denotes the best strategies of all other players $\{p_1, \dots, p_{i-1}, p_{i+1}, \dots, p_N\}$. Thus, $\pi_i(s_i, s_{-i}^*)$ denotes the reward obtained by player p_i when using strategy s_i in the context of other players using strategies s_{-i}^* , respectively [73, 74].

For each vehicle agent (i.e., player p_i) in the scenario, SAVVIDRIVER automatically extracts utility functions from the associated KAOS goal, k_i , to structure its respective reward function π_i (see Expression (7)). The reward function maps the utility functions to specific observable properties of the simulation platform, which is then used to guide and constrain the behavior of vehicles in the ITS simulation. Specifically, each KAOS goal model k_i contains a number M_i of utility functions f_{ij} associated with leaf-level goals, where $1 \leq j \leq M_i$. Each f_{ij} is a real-valued function (e.g., see Expression (4)) that maps a specific requirement of player p_i ’s goal model k_i to a satisficement value [29]. Each utility function associated with the leaf-level goals is assigned a weight value α_{ij} , $\alpha_{ij} \in \mathbb{R}$, denoting a developer-specified weight (e.g., to indicate the importance or impact) of the given goal. The reward function π_i directly guides and constrains the behavior of vehicles in the ITS simulation.

$$\pi_i(s_i) = \sum_{j=1}^{M_i} \alpha_{ij} \cdot f_{ij}(p_i). \quad (7)$$

875 **3.3 Step 3. Game-Based Testing**

876 This section overviews how SAVVIDRIVER integrates and operationalizes the KAOS
877 goal models and their utility functions into a game to explore human-based uncer-
878 tainty in an ITS simulation. An **ITS Simulator** is used to keep track of the operating
879 environment’s state for a given gaming process (see Figure 2, *ITS Simulator*). For each
880 timestep of a game, the following happens. First, agents use their respective strategies
881 to select actions (e.g., braking, throttle, steering, etc.) which are then provided as input
882 to the **ITS Simulator**. Second, the **ITS Simulator** executes the collective actions from
883 all the participating agents. The **ITS Simulator** then updates the environment (e.g.,
884 vehicle positions, velocities, etc.) and returns a new ITS state to the respective gaming
885 process. The sequence of each agent’s actions and resulting environment states inform
886 the RL learning process and may be archived (e.g., simulation traces) to support fur-
887 ther analysis processes. We next overview how SAVVIDRIVER uses game-based testing
888 in simulation to discover human-based uncertainty potentially impacting an Ego.
889

890 **Step 3a. NeV Training**
891

892 First, SAVVIDRIVER trains the NEV(s) to complete driving tasks while exhibiting a
893 specific driving style in the presence of the EGO (provided as input by a developer).
894 The NEV(s) are in training mode, where the DNN is actively learning new behavior
895 in response to its environment. The goal models from **Step 1b** inform the reward
896 structure of each NEV. Thus, the NEV(s) learn to complete their respective functional
897 goal specified in the corresponding KAOS goal model that reflects a particular driving
898 style (e.g., aggressive, distracted, timid, etc.). For example, an aggressive NEV may
899 exploit the safe driving behavior of an EGO (i.e., maintains a conservative following
900 distance) by cutting in front of the EGO in order to satisfy a NEV non-functional goal
901 to get to its destination quickly.

902
903 **Step 3b. AV Uncertainty Discovery**
904

905 Next, SAVVIDRIVER assesses the ability of the EGO to operate appropriately in the
906 presence of the trained NEV(s) (trained in **Step 3a**). The NEV(s) in *execution mode*
907 choose strategies learned during training (**Step 3a**) according to their reward func-
908 tions; they do not learn new behavior in response to agent interactions. During this
909 step, the EGO may exhibit previously unseen or unexpected behavior as it responds to
910 the other “human-operated” vehicles exhibiting different driving styles. For example,
911 when the aggressive NEV cuts off the EGO, the (unexpected) EGO response may be to
912 swerve to avoid a collision, which may lead to another collision. The result of this step is
913 a collection of *failure traces*, where *failure* is defined as a scenario execution where the
914 EGO did not reach its destination, for example, due to a collision with an NEV or a road
915 obstacle. Failure traces are sequences of agent actions and corresponding environment
916 states (i.e., trace data), indexed by timesteps, for a given execution of the mixed traffic
917 scenario where a failure occurs. Developers can use failure traces to visualize and replay
918 different executions of mixed traffic scenarios to better understand the interactions
919 and environment states that led to interesting behavior or unexpected EGO failures.

3.4 Step 4. AV Robustification	921
Similar to simulation-based testing [75, 76, 77], SAVVIDRIVER’s generated information (i.e., failure traces from Step 3b) can be used by developers to revise the system to prevent and/or mitigate the discovered unexpected EGO behavior. The information can be used in several ways, including updating system requirements, modifying system implementation, or used as training data for learning-enabled system components. We next elaborate on these approaches to robustification.	922 923 924 925 926 927 928 929 930 931 932 933 934 935 936 937 938 939 940 941 942 943 944 945 946 947 948 949 950 951 952 953 954 955 956 957 958 959 960 961 962 963 964 965 966
<i>Robustification of Software-Based AVs</i>	929
For traditional software-based EGOS (e.g., Intelligent Driving Model (IDM) [78]), developers can use failure traces to identify goal violations (e.g., collisions, failure to drive towards destination, etc.) and determine how to revise the behavior of the EGO. For example, developers may observe similar failures (i.e., collisions) during merge maneuvers when another vehicle is in close proximity to the EGO, resulting in low rewards. Developers can then use this collection of similar driving patterns/scenarios to specify goals that represent a “cautious” operating mode that increases the desired inter-vehicle distance to avoid collisions during merge maneuvers.	930 931 932 933 934 935 936 937 938 939 940 941 942 943 944 945 946 947 948 949 950 951 952 953 954 955 956 957 958 959 960 961 962 963 964 965 966
<i>Robustification of Learning-Based AVs</i>	929
For learning-based EGOS, SAVVIDRIVER supports robustification by retraining RL-based EGOS in the context of the discovered uncertainty (i.e., failure traces from Step 3b). During retraining, the EGO is in training mode and the NEV(s) are in execution mode. The EGO agent learns to complete the goals specified in its KAOS goal model in the presence of uncertainty posed by the NEV(s) that have learned to exhibit specific driving styles specified by their corresponding goal models. The result of this step is an automatically retrained EGO that can move robustly and safely, completing the given task in the presence of human-based uncertainty exhibited by the NEV.	930 931 932 933 934 935 936 937 938 939 940 941 942 943 944 945 946 947 948 949 950 951 952 953 954 955 956 957 958 959 960 961 962 963 964 965 966
4 Demonstration	950
To demonstrate the use of the SAVVIDRIVER framework to discover unexpected human-based behavior(s) and assess EGO responses, we have applied it in several proof-of-concept use cases based on real-world traffic accident data [30, 79, 80, 81]. We present results for the discovered mixed traffic interactions that cause EGO failure, and then illustrate how developers can use these results to improve an EGO’s robustness in response to the human-based uncertainty.	951 952 953 954 955 956 957 958 959 960 961 962 963 964 965 966
<i>Experiment Setup</i>	958
Our demonstration is intended as a proof-of-concept study to illustrate the modeling, uncertainty discovery, and robustness analysis capabilities of our framework. To this end, we leverage existing tooling for our experiments. First, we use our custom in-house simulation package, TinyRoad [7], to provide a light-weight 2D traffic environment. TINYROAD uses a bicycle-kinematics physics model [82] and simple 2D graphics that require less computational overhead when compared to more sophisticated and computationally expensive simulation platforms (e.g., CARLA [39], Gazebo [83]). Thus,	959 960 961 962 963 964 965 966

967 the selected simulation platform supports quick training and evaluation of RL agents
 968 while preserving the key behavioral characteristics of EGO and NEV interactions.

969 While SAVViDRIVER can use any RL algorithm that takes as input the environmental state and outputs a discrete action for the vehicle, we use PPO [16] and the
 970 OpenAI Gym [84] libraries to implement RL training and agents within the simulation
 971 as a proof-of-concept demonstration for SAVViDRIVER. We implement a custom environment using the Stable Baselines3 library. The observation space comprises sensor
 972 inputs; in this work, we use image-based observations of size $\mathbb{R}^{128 \times 128 \times 3}$. The images
 973 are processed by a Convolutional Neural Network (CNN), and the resulting vector is
 974 then passed to a multi-layer perceptron (MLP) that outputs a distribution over the
 975 action space. The action space is a vector in $\{x_1, x_2 : x_1, x_2 \in [-1, 1]\}$ where the first
 976 component represents throttle values and the second component represents steering
 977 values. Table 2 overviews the hyperparameters used in PPO training. We started with
 978 hyperparameter values commonly used in other DRL settings [16] and empirically
 979 tuned them for our application.
 980

981
 982 **Table 2:** Overview of RL training parameters.
 983

Hyperparameters	Value	Hyperparameters	Value
Total timesteps	3×10^6	Clip ϵ	0.1
Early convergence	True	Entropy Coefficient	0.02
Optimizer	Adam	Learning Rate	1×10^{-4}
Discount Factor γ	0.99	Replay Buffer Size	2048

990
 991
992 Evaluation Metrics

993 We use two well-established and commonly-used vehicle safety indicators to assess the
 994 performance of the EGO: the Average Failure Rate (AFR) [85] and the average Time
 995 Exposed Time-to-collision (TET) [86, 87]. The safety metrics are defined over a set of
 996 episodes E , where $|E| = 100$ in each use case. An episode is an execution of the mixed
 997 traffic simulation from an initial state to a terminal state (i.e., the EGO reaches its
 998 destination or a collision occurs).
 999

1000 In our studies, a *failure* is defined as an episode where the EGO under study does
 1001 not reach the destination, for example, due to a collision between the EGO under study
 1002 and an NEV or a road obstacle. Expression (8) defines an indicator function δ_{AFR} that
 1003 evaluates to 1 if a failure occurs, and 0 otherwise. The AFR metric is defined as the
 1004 average number of collisions observed over episode set E (see Expression (9)).
 1005

$$1006 \quad \delta_{\text{AFR}}(e) = \begin{cases} 0 & \text{if } \text{EGO.state} \neq \text{reach_dest} \\ 1 & \text{if } \text{EGO.state} = \text{reach_dest} \end{cases} \quad (8)$$

$$1007 \quad \text{AFR}(E) = 100 \times \frac{1}{|E|} \sum_{e \in E} \delta_{\text{AFR}}(e) \quad (9)$$

The Time-to-Collision (TTC) metric [87] is defined as the time remaining until a collision occurs, where collisions are predicted using the linear projection of each vehicle's future position [85]. Expression (10) defines the TTC value for an AV belonging to vehicle set \mathcal{I} at a given timestep t . The distance formula d calculates the predicted Euclidean distance between the position $pos_{AV}(t + \tilde{t})$ of the AV, and the position $pos_j(t + \tilde{t})$ of vehicle $p_j, p_j \in \mathcal{I} - AV$ at future time $t + \tilde{t}$. When no collision is predicted, the TTC value is set to ∞ [85].

$$TTC(Ego, \mathcal{I} - Ego, t) = \min (\{\{\tilde{t} \geq 0 \mid d(pos_{AV}(t + \tilde{t}), pos_j(t + \tilde{t})) = 0\} \cup \{\infty\}\}), \forall j \in \mathcal{I} - Ego. \quad (10)$$

Next, Expression (11) defines an indicator function δ_{TET} that evaluates to 1 if an input value ttc is less than or equal to the given time threshold (seconds) $\tau, \tau \in \mathbb{R}$, and 0 otherwise. Finally, the TET metric is defined as the duration the EGO was exposed to a TTC value below some threshold τ during episode e 's time interval $\{0, t_e\}$, averaged over episode set E (see Expression (12)) [85, 86].

$$\delta_{TET}(ttc) = \begin{cases} 0 & \text{if } ttc > \tau \\ 1 & \text{if } ttc \leq \tau \end{cases} \quad (11)$$

$$TET(E) = \frac{1}{|E|} \sum_{e \in E} \left(\frac{1}{t_e} \sum_{t=0}^{t_e} \delta_{TET}(TTC(Ego, \mathcal{I} - Ego, t)) \right) \quad (12)$$

4.1 Use Case: Left Turn

Our first use case explores an uncontrolled left turn intersection. According to the NHTSA [88], a left-turn maneuver is one of the most frequent pre-crash events, especially at intersections without controlled signals [79, 80]. Figure 7a provides an overview of the left-turn use case considered, where the blue EGO seeks to make a left turn and the orange AGGRESSIVE-NEV and green DISTRACTED-NEV are traveling in the left lane (towards the blue EGO). Figure 7b provides the corresponding goal model for the green DISTRACTED-NEV.

Data

This section describes the key information that is used to define the scenario for this use case. The *scenario* is an unprotected left-turn intersection that comprises a two-lane road with a perpendicular road connecting to the left lane. Therefore, a vehicle in the right lane attempting to make a left turn must cross a lane with oncoming traffic. The *agents* participating in this scenario are an aggressive driver (orange), a distracted driver (green), and the AV (blue). The AV under study uses a traditional IDM for decision-making. The *road layout* is modeled based on real-world map data, and we provide the road geometry as input to SAVVIDRIVER.

1059 ***Step 1. Modeling***

1060 This section describes the development of goal models (**Step 1. Modeling**) for our
 1061 left-turn use case. We explore two different NEVs, an AGGRESSIVE-NEV and a
 1062 DISTRACTED-NEV operating in a multi-agent setting. For the AGGRESSIVE-NEV,
 1063 we reference the component library to reuse the non-functional subtree of the
 1064 AGGRESSIVE-NEV defined in our merge running example (see Section 3). The pre-
 1065 viously developed non-functional subtree is based on NHTSA’s traffic data that
 1066 identifies three leading causes of accidents related to aggressive drivers: speeding, prox-
 1067 imity to other road users, and inability to center in a lane [24, 25, 26]. We update
 1068 the functional objective of the AGGRESSIVE-NEV to reflect the functional context-
 1069 dependent goal: NEV-G7 ‘stay in right lane of roadway’. This process demonstrates
 1070 how SAVVIDRIVER facilitates the reusability of goal models by using previously
 1071 defined agent goal(s) in a new scenario. Figure 7b shows the KAOS model for the
 1072 DISTRACTED-NEV, where the top-level goal of NEV-G1 ‘arrive at destination’ is
 1073 decomposed into subgoals such as NEV-G8 ‘driver enters distracted state’, NEV-
 1074 G6 ‘lane swerving’, and NEV-G4 ‘drive in close proximity to other vehicles’.

1075

1076

1077

1078

1079

1080

1081

1082

1083

1084

1085

1086

1087

1088

1089

1090

1091

1092

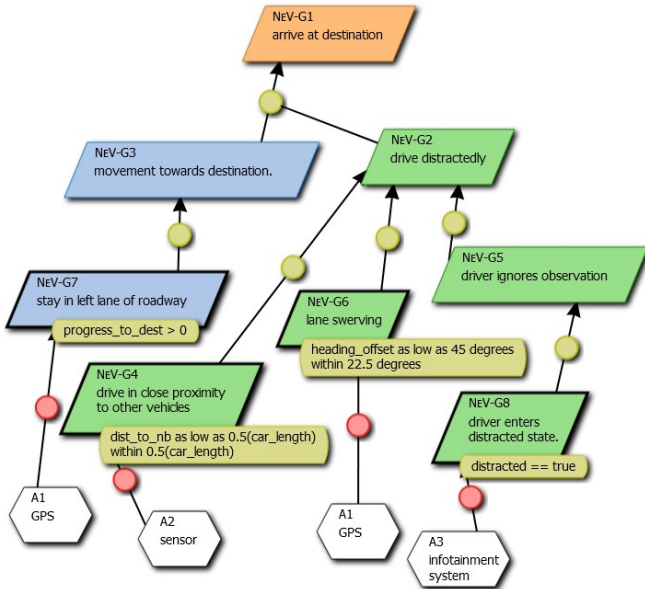
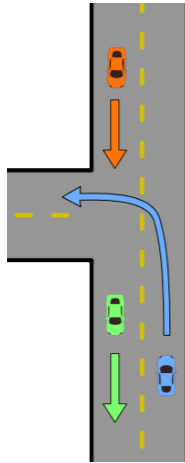
1093

1094

1095

1096

1097 (a) Graphical depiction of
 1098 left-turn use case.



(b) KAOS goal model for the green DISTRACTED-NEV.

1099 **Fig. 7:** Overview of left-turn use case and green DISTRACTED-NEV goal model. The
 1100 left-turn use case involves three vehicles. The blue EGO attempts to make a left turn,
 1101 while the orange AGGRESSIVE-NEV and green DISTRACTED-NEV are driving in the
 1102 left lane.

1103

1104

Step 2. Middleware	1105
This section describes how SAVVIDRIVER processes goal models and scenario information to automatically initialize the gaming setup and simulator for the left-turn use case. First, Step 2a takes as input the scenario definition file that captures key context-dependent information for this use case and instantiates the simulator. Next, the reward function for each agent is automatically compiled from the aggregate utility functions in their respective goal models (Step 2b). Listing 2 provides a pseudocode example of the automatically generated reward function for the DISTRACTED-NEV. The utility function associated with goal NEV-G4 rewards the DISTRACTED-NEV for driving as close as possible to other vehicles, with a maximum reward assigned when its distance to the closest vehicle is less than half of its length. The utility function associated with NEV-G6 rewards the DISTRACTED-NEV for swerving and is parameterized by the current heading offset from the lane center. The maximum reward is achieved when the current offset is greater than 45 degrees. The utility function associated with NEV-G8 rewards the DISTRACTED-NEV for entering a distracted state and is parameterized by a boolean value that indicates if the driver is distracted. The NEV-G8 utility function returns a reward of 1 if the driver is distracted and 0 otherwise. The NEV-G7 rewards the DISTRACTED-NEV for making progress between timesteps. The NEV-G7 utility function returns a reward of 1 if the driver makes progress and 0 otherwise. Each utility function evaluates to a real-valued number (i.e., level of satisfaction). Using Expression (7), the reward is computed as the linear weighted sum of the satisfaction values multiplied by developer-specified weights. Since the AGGRESSIVE-NEV has the same non-functional objectives as the merge running example, we regenerate the AGGRESSIVE-NEV’s reward structure to reflect the new context-dependent functional objective for the left-turn use case. We describe the results for the left-turn use case next.	1106 1107 1108 1109 1110 1111 1112 1113 1114 1115 1116 1117 1118 1119 1120 1121 1122 1123 1124 1125 1126 1127 1128 1129 1130 1131 1132 1133 1134 1135 1136 1137 1138 1139 1140 1141 1142 1143 1144 1145 1146 1147 1148 1149 1150
Step 3. Game-Based Testing	1132
Figure 8 illustrates a failure scenario observed during the uncertainty discovery process (Step 3b) for the left-turn use case. The blue EGO’s initial attempt to make a left-turn maneuver (see (A), Figure 8) is aborted due to the swerving behavior of the green DISTRACTED-NEV. Then the blue EGO attempts another left-turn maneuver in close proximity to the orange AGGRESSIVE-NEV, causing it to enter the EGO’s lane (see (B), Figure 8). The orange AGGRESSIVE-NEV’s behavior causes the blue EGO to accelerate and collide with the road barrier (see (C), Figure 8), therefore resulting in an increased failure rate when the two NEVs are in close proximity to the EGO’s lane. Table 3 provides quantitative results for the left-turn use case. In the absence of the NEVs, the EGO is able to complete the left turn with a failure rate of approximately 0.00%. However, when exposed to the distracted and aggressive NEVs, the EGO’s failure rate increases to 12.00%. Additionally, the observed TET values in Table 3 indicate that the EGO was exposed for the highest average duration of time to critical TTC values τ , $\forall \tau \in \{1, 2, 3\}$ in the presence of the NEVs. TTC values below a specific time threshold (e.g., $\tau = 3$ seconds [86]) potentially indicate that a vehicle would not have enough time to perform a collision-avoiding maneuver, such as applying the	1133 1134 1135 1136 1137 1138 1139 1140 1141 1142 1143 1144 1145 1146 1147 1148 1149 1150

1151 brakes to stop the vehicle. We observe higher average TET values indicating the EGO
1152 was in a near-collision state when exposed to both NEVs.

1153

1154 Listing 2: Pseudocode for the DISTRACTED-NEV’s reward function corresponding
1155 to its KAOS goal model.
1156

```
1157 1 def reward(p):
1158 2     # utility function for G4
1159 3     # p.nb := distance to nearest neighbor
1160 4     # p.s := car length of NeV
1161 5     fi_0 = (0 if p.nb >= 0.5*p.s else
1162 6         (1 if p.nb < 0.5*p.s else
1163 7             (0.5*p.s-p.nb)/0.5))
1164 8
1165 9     # utility function for G6
116610     # p.hof := NeV's heading offset from current lane
116611     fi_1 = (0 if p.hof <= 22.5 else
116612         (1 if p.hof >= 45 else (45-p.hof)/22.5))
116713
116814     # utility function for G8
116915     # p.d := boolean indicating if NeV is distracted
117016     fi_2 = (0 if not p.d else 1)
117117
117218     # utility function for G7
117319     # p.prog := percent increase in route completion from last update
117320     fi_3 = (1 if p.prog > 0 else 0)
117421
117522     # weights - default is equal weights
117523     alpha = [1, 1, 1, 1]
117624
117725     # Reward function (see Expression (4))
117826     uf = [fi_0, fi_1, fi_2, fi_3]
117927     reward = 0
118028     for j in range(|uf|):
118129         reward += alpha[j]*uf[j]
118230     return reward
```

1183 *Step 4. Robustification (of Software-based Ego)*

1184 The discovered uncertainty and corresponding failure traces are used to inform a
1185 reconfiguration of the EGO’s IDM, a rule-based controller. Specifically, during the
1186 replay and analysis of the failure traces, we observed that the EGO did not properly
1187 wait for an opening to make a left turn, attempting the turning maneuver in close
1188 proximity to other vehicles. We confirmed our visual observations through further
1189 examination of the failure trace data, specifically the distance between the vehicles
1190 leading up to a failure. Informed by our analysis, we developed a KAOS functional
1191 subtree for ‘cautious’ mode [89] for the EGO that implemented a blocking routine until
1192 the intersection is clear with respect to a given distance threshold before attempting to
1193 perform the left-turn maneuver. After reconfiguration in **Step 4. Robustification**,
1194 the robustified EGO is better able to wait for openings in the intersection, thereby
1195 reducing its failure rate from 12.00% down to 1.00%. This use case demonstrated
1196

how SAVVIDRIVER was able to reuse existing goal models, extend them with different numbers and types of drivers, apply them to a new ITS use case to discover unexpected human behavior with the corresponding unexpected EGO responses, and then use this information to reconfigure the EGO, resulting in a reduced failure rate. Importantly, no low-level simulation code was modified to explore this robustification process.

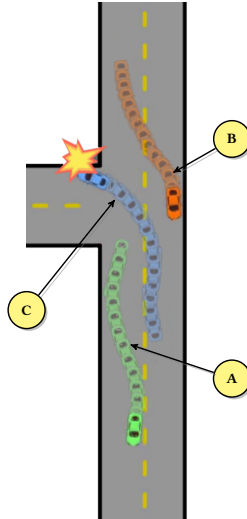


Fig. 8: Left turn use case overview. The green DISTRACTED-NEV’s sporadic movement led to a preemptive turn in the blue Ego. The Ego then speeds up to avoid collision with the orange AGGRESSIVE-NEV, resulting in a crash of the Ego.

Table 3: Evaluation of *AFR* and *TET* metrics for the left-turn case study, where red color indicates the worst value for each metric. A higher AFR indicates a higher average collision rate and a higher TET indicates higher average time spent in a near-collision state (i.e., predicted time-to-collision less than τ seconds).

Setting	AFR	TET		
		$\tau = 1\text{s}$	$\tau = 2\text{s}$	$\tau = 3\text{s}$
Base AV	0.00%	0.00%	0.00%	0.50%
Uncertainty Discovery	12.00%	2.90%	3.80%	4.90%
Robustified AV	1.00%	0.10%	0.80%	2.70%

1243 **4.2 Use Case: Weave Lane**

1244 Our next use case explores a weave lane highway merge. Figure 9 provides a graphical
1245 depiction of the weave lane highway merge use case, where the blue EGO is trailed by
1246 the orange NEV. Both vehicles must exit the on-ramp and merge onto the highway. A
1247 weave lane is a challenging highway merge scenario, as vehicles entering the highway
1248 often start at a low speed due to the entrance curve speed limit and can cause auto-
1249 mated vehicles to fault [30]. For example, a 2020 Waymo EGO exhibited unexpected
1250 behavior during a highway merge scenario where the EGO failed to complete the merge
1251 maneuver [81]. We next detail how SAVVIDRIVER is used to model and explore specific
1252 human-based behaviors that may lead to vehicle failures in the weave lane scenario.
1253

1254

1255

1256

1257

1258

1259

1260

1261

1262

1263

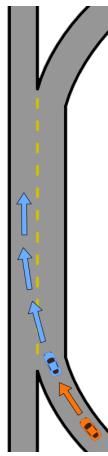
1264

1265

1266

1267

1268



1269 **Fig. 9:** A scenario capturing the weave lane use case in TINYROAD. Both the EGO
1270 and AGGRESSIVE-NEV are traveling from an on-ramp and attempt to merge onto the
1271 highway.

1272

1273

1274

1275 **Data**

1276 Using historical data and/or domain expertise, we identify three types of information
1277 required for SAVVIDRIVER and capture them in a scenario definition. The *scenario* is
1278 a weave lane that comprises a highway on-ramp that merges onto the main lane of the
1279 highway. The *agents* participating in this scenario are the AGGRESSIVE-NEV and the
1280 EGO. In contrast to the left-turn use case, this use case explores an EGO that uses an
1281 RL-based controller for decision-making that was trained to satisfy the requirements
1282 captured in the goal model shown in Figure 6a [7]. The *road layout* is modeled based
1283 on real-world map data, and we provide the road geometry as input to SAVVIDRIVER.
1284

1285

1286

1287

1288

Step 1. Modeling	1289
This section describes the development of goal models for the weave lane use case. Since the non-functional objectives describe <i>how</i> an agent should achieve a task, they can often be reused between different driving scenarios. In this use case, we reuse the non-functional subtrees saved in our Component Library for both the AGGRESSIVE-NEV and EGO. For both agents, we update their functional objective to reflect the context-dependent top-level function goal: ‘merge onto highway’. This process illustrates how a developer may leverage the Component Library during Step 1. Modeling to reuse existing context-independent non-functional subtrees and apply them in a new scenario to discover additional sources of human-based uncertainty.	1290 1291 1292 1293 1294 1295 1296 1297 1298 1299 1300 1301 1302 1303 1304 1305 1306 1307 1308 1309 1310 1311 1312 1313 1314 1315 1316 1317 1318 1319 1320 1321 1322 1323 1324 1325 1326 1327 1328 1329 1330 1331 1332 1333 1334
Step 2. Middleware	1300
In this step, SAVVIDRIVER processes goal models and scenario information to automatically initialize the gaming setup and simulator for the weave lane use case. Step 2a processes the scenario definition file and instantiates the simulator. Next, the goal models are automatically processed to generate the reward structure for the game-based testing process (Step 2b). Specifically, utility functions associated with leaf-level goals are aggregated into a linear weighted sum that represents the reward for each agent in the game. Notably, SAVVIDRIVER automatically generates a new reward structure for the weave lane use case through model-level updates rather than low-level simulation code changes.	1301 1302 1303 1304 1305 1306 1307 1308 1309 1310 1311 1312 1313 1314 1315 1316 1317 1318 1319 1320 1321 1322 1323 1324 1325 1326 1327 1328 1329 1330 1331 1332 1333 1334
Step 3. Game-Based Testing	1311
Figure 10 illustrates an EGO failure observed during the uncertainty discovery phase. In the presence of the NEV, the EGO attempted an early merge maneuver onto the highway to maintain a safe distance away from the AGGRESSIVE-NEV. However, the EGO failed to account for the trajectory of the NEV, resulting in an increased failure rate when both vehicles merged in close proximity to each other. Table 4 shows a comparison between the average EGO AFR and TET over 100 random episodes. In this use case, we use an AV that has been trained with an RL as a baseline. The baseline EGO is able to complete the highway merge in the presence of external rule-following traffic with a failure rate of only 2.0%. However, when exposed to the aggressive NEV (Step 3b), the EGO’s failure rate increases to 34.0%. Additionally, the observed TET values (see Table 4) indicate that the EGO was exposed for the highest average duration of time to critical TTC values (i.e., τ , $\forall \tau \in \{1, 2, 3\}$) in the presence of the aggressive NEV. Higher average TET values indicate the EGO was more frequently exposed to near-collision scenarios, which may contribute to the increased failure rate. For example, we observe that the EGO was in a near-collision state (within $\tau = 3$ seconds) for 12.60% of the episodes when exposed to the aggressive NEV.	1312 1313 1314 1315 1316 1317 1318 1319 1320 1321 1322 1323 1324 1325 1326 1327 1328 1329 1330 1331 1332 1333 1334

1335
1336
1337
1338
1339
1340
1341
1342
1343
1344
1345
1346
1347
1348



1349 **Fig. 10:** Demonstration of a failure discovered by SAVVIDRIVER, where the orange
1350 AGGRESSIVE-NEV completes its merge before the blue EGO and speeds up, causing
1351 a collision as the EGO tries to merge.

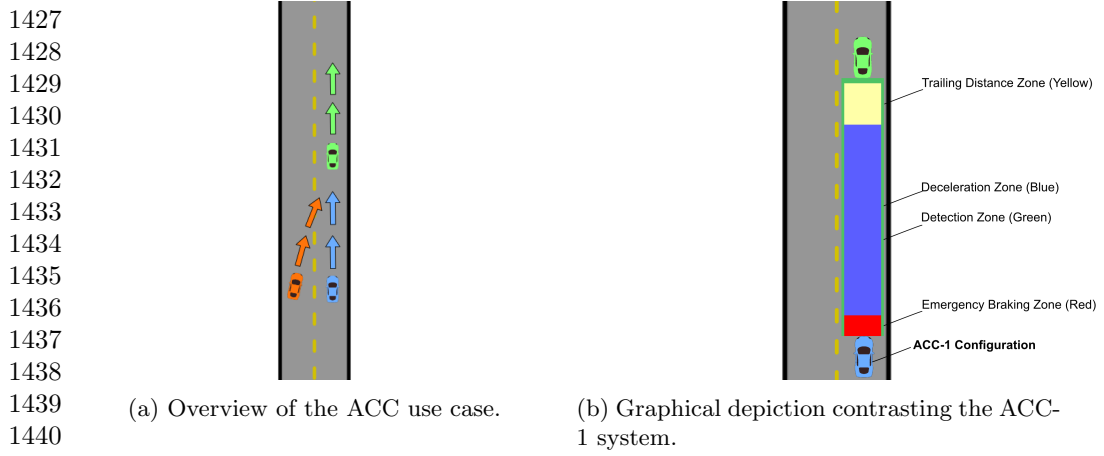
1352
1353
1354
1355
1356
1357
1358

Table 4: Evaluation of *AFR* and *TET* metrics for the weave lane case study, where
1355 red color indicates the worst value for each metric. A higher *AFR* indicates a higher
1356 average collision rate and a higher *TET* indicates higher average time spent in a near-
1357 collision state (i.e., predicted time-to-collision less than τ seconds).

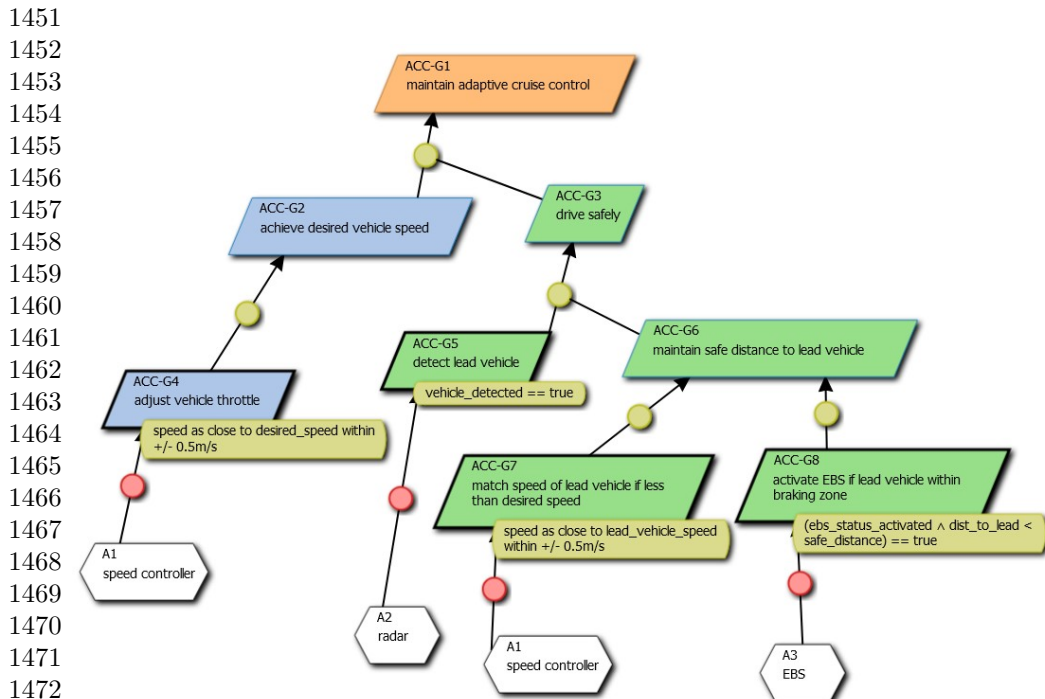
Setting	AFR	TET		
		$\tau = 1s$	$\tau = 2s$	$\tau = 3s$
Base AV	2.00%	4.20%	7.50%	7.90%
Uncertainty Discovery	34.00%	8.60%	11.40%	12.60%
Robustified AV	18.00%	5.00%	7.10%	8.00%

1366
1367
1368 **Step 4. Robustification (of RL-based Ego)**
1369
1370
1371
1372
1373
1374
1375
1376
1377
1378
1379
1380

4.3 Use Case: Adaptive Cruise Control	1381
Our final use case explores a merge scenario involving an AV equipped with a traditional software implementation of an Adaptive Cruise Control (ACC) system, an Advanced Driver Assistant System (ADAS) feature found in most modern vehicles.	1382
The ACC system uses onboard sensors, such as radar and lidar, to maintain a safe trailing distance between itself and a <i>target</i> vehicle. The goal of this use case is to illustrate how SAVVIDRIVER may be used to assist in the engineering, assessment, and manual reconfiguration of ADASs (i.e., ACC) by developers. Figure 11a shows the road and vehicle configuration for the ACC scenario. An orange NeV seeks to merge into the lane of the blue EGO AV before reaching the end of the road. The AV seeks to maintain a safe trailing distance to a green target vehicle traveling at a constant speed.	1383
	1384
	1385
	1386
	1387
	1388
	1389
	1390
	1391
	1392
	1393
	1394
	1395
	1396
	1397
	1398
	1399
	1400
	1401
	1402
	1403
	1404
	1405
	1406
	1407
	1408
	1409
	1410
	1411
	1412
	1413
	1414
	1415
	1416
	1417
	1418
	1419
	1420
	1421
	1422
	1423
	1424
	1425
	1426



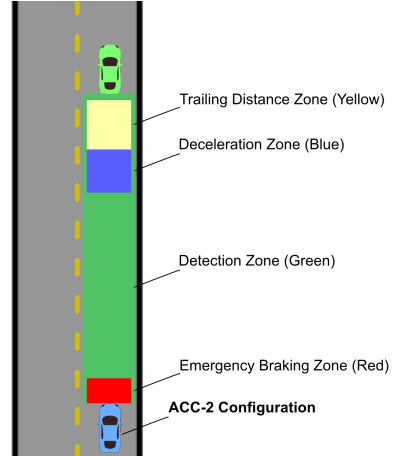
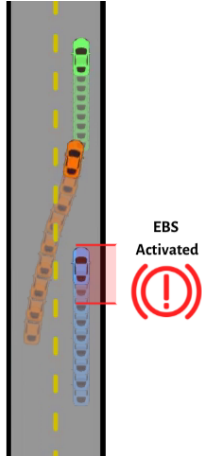
1442 **Fig. 11:** Overview of the ACC use case and the ACC-1 system. Subfigure (a) shows
1443 the ACC use case that involves three vehicles. The green NeV target vehicle travels
1444 straight at a constant speed. The blue EGO vehicle uses a rule-based ACC controller to
1445 maintain a fixed trailing distance to the vehicle in front. The orange AGGRESSIVE-NEV
1446 seeks to merge into the right lane. For Subfigure (b), the yellow box shows the trailing
1447 distance the ego vehicle aims to maintain. The green box denotes the distance when
1448 the ego vehicle detects the green non-ego target vehicle. The blue box indicates the
1449 deceleration zone. Finally, the red box denotes the emergency braking zone, where the
1450 ego vehicle applies the maximum braking force if an object is detected within the zone.



32
Fig. 12: KAOS model for ACC subsystem.

<i>Step 2. Middleware</i>	1473
Similar to the previous use cases, SAVVIDRIVER automatically instantiates the simulation environment, gaming setup, and compiles the reward function for each agent using the aggregate utility functions from their respective goal models. We next describe the game-based testing and discovered uncertainty for the ACC use case.	1474 1475 1476 1477 1478
<i>Step 3. Game-Based Testing</i>	1479
Figure 13a illustrates a critical scenario observed during uncertainty discovery. The orange AGGRESSIVE-NEV suddenly merges in front of the blue EGO, causing the ACC system to activate its EBS. Table 5 shows a comparison between the average duration(s) of EBS activation over 100 random episodes. In the baseline scenario, the EGO does not activate its EBS as it follows the target vehicle. However, when exposed to the AGGRESSIVE-NEV, the average EBS duration increases from 0.00 seconds to 3.52 seconds. This increase indicates the ACC experienced more near-collision events in the presence of the AGGRESSIVE-NEV.	1480 1481 1482 1483 1484 1485 1486 1487 1488
<i>Step 4. Robustification (of ADAS subsystem)</i>	1489
Observing the unexpected maneuver from the AGGRESSIVE-NEV and response from the EGO configured with ACC-1, a developer can engineer or reconfigure the ACC system, yielding an alternative ACC-2 controller to mitigate the unsafe scenario in Step 4. Robustification . Figure 13b shows an overview of the ACC-2 configuration. In contrast to the gradual deceleration when a target vehicle is detected by the ACC-1 controller (see Figure 11b), the ACC-2 controller’s behavior is revised to maintain its speed until it reaches a short deceleration zone before applying the brakes to match the speed of the target vehicle (see Figure 13b). After robustification, the average duration of EBS activation over 100 episodes decreases to 0.16 seconds in the presence of the AGGRESSIVE-NEV. As such, this use case highlights how a developer may use SAVVIDRIVER to identify problems in an initial configuration of an ACC controller, engineer a mitigating solution, and confirm the solution addresses previously identified unexpected behaviors. The reconfiguration of the ACC system demonstrated in this use case captures a real-world use case when ACC systems were initially deployed in the early 2000s by OEMs. ³ First iterations of ACC systems applied a similar configuration as our ACC-1 system. As OEMs discovered that aggressive drivers may cut off the ADAS-equipped vehicles, they changed the behavior of their ACC models to apply the brakes as they enter the “short deceleration zone” of the target vehicle (i.e., ACC-2). This example shows that by applying SAVVIDRIVER, developers can identify unsafe situations during testing and modify the behavior of their system to mitigate similar situations.	1490 1491 1492 1493 1494 1495 1496 1497 1498 1499 1500 1501 1502 1503 1504 1505 1506 1507 1508 1509 1510 1511 1512 1513 1514 1515 1516 1517 1518
5 Discussion	1512
This section discusses our results, including key findings and envisioned usage scenarios.	1513

³This information is based on data provided by our industrial collaborators.



1519
1520
1521
1522
1523
1524
1525
1526
1527
1528
1529
1530
1531
1532
1533 (a) Example trajectory of the orange
1534 AGGRESSIVE-NEV who abruptly merged
1535 in front of the blue EGO, activating the
1536 EBS of the EGO.

1533 (b) Graphical depiction contrasting the
1534 ACC-2 system. This configuration main-
1535 tains a smaller trailing distance compared
1536 to ACC-1.

1537
1538 **Fig. 13:** Overview of (a) sample uncertainty discovered by SAVVIDRIVER and (b) the
1539 corresponding robustified EGO configuration.

1540
1541

1542 **Table 5:** Evaluation of ACC use case, where red color indicates the worst value for the
1543 EBS duration metric. A higher EBS duration indicates a higher average time spent in
1544 a near-collision state.

	Setting	EBS Duration (s)
1547	Base AV (ACC-1)	0.00
1548	Uncertainty Discovery	3.52
1549	Robustified AV (ACC-2)	0.16

1551
1552
1553 **5.1 Synergizing Game Theory, Reinforcement Learning, and**
1554 **Goal Modeling**

1556 This paper has shown that game theory and RL can be synergistically combined for
1557 uncertainty exploration in AV testing. While existing research has explored coop-
1558 erative game theory to assess how AVs and human-driven vehicles may cooperate
1559 to improve a common goal (e.g., improve traffic flow), these studies do not reflect
1560 the challenges of AVs when deployed, where they must successfully navigate scenar-
1561 ios with other human-driven vehicles that cannot communicate or share intentions.
1562 Other work has explored adversarial agents, where the objective is to minimize the
1563
1564

reward of the AV under study. SAVVIDRIVER leverages non-cooperative game theory to model a traffic scenario, where players of the game (i.e., different vehicles) do not explicitly communicate, form coalitions, nor share high-level rewards. By defining high-level functional objectives (i.e., the objective associated with the scenario) and the non-functional objectives (i.e., how the vehicles shall achieve those objectives), our approach discovers maneuvers that can lead to undesirable outcomes.

To the best of our knowledge, SAVVIDRIVER is the first to integrate goal-based modeling with game theory and RL in order to address modularity and reuse in the discovery of human-based uncertainty. Existing research has explored the modeling of environmental uncertainty (e.g., raindrops, lighting conditions, etc.), where developers may have explicit *a priori* models (e.g., physics-based solutions, simulations, etc.) for capturing and generating samples of uncertainty [92]. However, there is not an explicit modeling approach that captures the broad range of epistemic uncertainty posed by interactions with different types of external human drivers. Instead, a key contribution of this work is the use of game theory and RL to automatically generate manifestations of human-based uncertainty based on declarative specifications of driver behaviors. SAVVIDRIVER’s goal models provide developers with a means to systematically decompose objectives into sub-objectives, each of which can be further refined down to the level of requirements. Those goal models comprise modular subtrees that can then be reused and/or recombined with existing goal models to form new external vehicle objectives that produce novel human-based behaviors and unexpected responses from the AV. For example, in the Weave Lane use case, we demonstrate modularity by combining the context-independent non-functional subtrees for aggressive behavior with a new functional subtree corresponding to the ‘merge onto highway’ top-level function objective. During the design phase, automotive developers can archive a collection of goal models corresponding to human-based driving behaviors, and reuse them to explore the impact of human-based uncertainty in a broad range of traffic scenarios/operating contexts. For example, in the ACC use case, we demonstrated reuse of the AGGRESSIVE-NEV goal model from our running example in a merge scenario involving a new type of EGO (ACC-1 and ACC-2 systems). By decoupling functional and non-functional objectives via reusable and modular goal models, developers can explore different dimensions of human-based uncertainty through the manipulation of high-level models rather than low-level code. We quantify the ability to generate uncertainty by assessing the EGO’s behavior when interacting with external vehicles controlled by SAVVIDRIVER’s automatically-discovered NEV behavior models. An EGO failure denotes epistemic doubt (due to uncertainty) in the EGO software under study as it is not able to handle the previously unseen contexts. We showed how developers can leverage those samples of epistemic uncertainty to reduce epistemic gaps in the AV’s behavior through robustification techniques, including the reconfiguration of AV software/requirements.

5.2 Experimental Findings and Applications

The results of the SAVVIDRIVER framework (i.e., failure traces corresponding to human-based uncertainty) can be used in several ways by stakeholders, including AV robustification to human-based uncertainty, revision/addition of requirements, and

1611 may even inform regulatory changes. For each use case, the input Ego software ini-
1612 tially appeared to have safe behavior with low failure rates. We demonstrated that
1613 SAVVIDRIVER can be used to train RL-based NEV agents that caused undesirable
1614 behaviors in the input EGOS, leading to a significant increase in failure rates when
1615 exposed to the discovered uncertainty. Finally, we showed several different robustifi-
1616 cation approaches across our use cases, where the result of the robustification step
1617 was an EGO that could mitigate uncertainty, thereby reducing its failure rates when
1618 interacting with the discovered NEV behaviors. For learning-based AVs, those fail-
1619 ure traces may be used as supplemental training data to improve the robustness of
1620 the AV to the discovered uncertainty. For example, in the Weave Lane use case (see
1621 Section 4.2), we demonstrated how retraining the learning-based EGO in the pres-
1622 ence of the aggressive NEV improved the EGO’s performance, reducing the AFR by
1623 16.00%, and reducing the TET by approximately 4.00%. In the Left Turn and ACC
1624 use cases (see Section 4.1 and Section 4.3, respectively), we demonstrated how the dis-
1625 covered failure traces could be used by developers to revise the EGO’s requirements
1626 (and concrete implementation), resulting in reduced AFR and EBS duration, respec-
1627 tively. The discovered failure traces may also be used by regulatory agencies and/or
1628 civil engineers to improve roadway safety. For example, in the Left Turn use case,
1629 the discovered human-based uncertainty may inform the addition of traffic lights/stop
1630 signs to the uncontrolled intersection to prevent similar failures in the real world.

1631 SAVVIDRIVER provides developers with a means to model driver behavior and
1632 discover human-based uncertainty in simulation. While we used our custom in-house
1633 simulator (i.e., TINYROAD) as a proof-of-concept, SAVVIDRIVER is not directly cou-
1634 pled to a specific simulation platform. Automotive developers and domain experts
1635 can leverage high-fidelity in-house tooling to instantiate specific scenarios and use
1636 SAVVIDRIVER to discover potential faults in the design of both the vehicle software
1637 and/or roadway infrastructure. Using high-fidelity simulators, developers can explore
1638 variations of vehicle objectives (i.e., leveraging SAVVIDRIVER’s modular goal mod-
1639 els), vehicle types (e.g., truck, motorcycle, SUV, etc.), and/or operating contexts (e.g.,
1640 highway ramp merge) to explore different dimensions of human-based uncertainty. By
1641 assessing the AV’s interaction with different types of drivers in a range of road con-
1642 figurations, SAVVIDRIVER can identify edge cases and other undesirable interactions
1643 before deployment, thereby facilitating revisions to the requirements, addition of new
1644 requirements, or updates to the system under study.

1645

1646 **6 Related Work**

1647

1648 This section overviews related work relevant to SAVVIDRIVER. First, we discuss related
1649 work with game theory and RL. Next, we discuss relevant research for game-based
1650 testing of AVs. Finally, we overview other model-based approaches to RL, uncertainty
1651 discovery, or AVs.

1652 A number of researchers have proposed game theory or RL-based approaches to
1653 train AV logic or improve the robustness of AVs against uncertainty. Liniger *et al.* [52]
1654 proposed a non-cooperative game theory approach to train agents for autonomous
1655 racing games, but uses the same reward objective for all agents (i.e., agents compete
1656

towards the same goal). Cao *et al.* [17] proposed an imitation learning approach to learn different types of driving models for an AV, and uses RL to learn to swap between the different learned policies. Li *et al.* [93] proposed a cooperative game-theoretic approach to model driver and vehicle interactions, but do not consider human-based uncertainty using a non-cooperative setting and have strictly defined reward functions for RL. Gupta *et al.* [18] introduced a framework to train two dueling agents in an RL setting, training a resilient ego vehicle against a (possibly adversarial) non-ego agent. Zhou *et al.* [94] proposed the UBRL framework, identifying potentially unreliable decisions of an RL agent, but does not account for human-induced uncertainty. Chan *et al.* [7] demonstrated that RL and non-cooperative game theory can be combined to discover undesirable AV behaviors. However, existing works largely use ad hoc development approaches to structure game objectives and/or traffic scenarios. Our work uses goal models to explicitly capture the functional/non-functional objectives of different driving styles and provides a reusable approach to explore human-based uncertainty for AVs through gaming and RL.

Game-based testing has been used to assess and/or improve AVs with respect to uncertainty posed by other drivers. Liu *et al.* [15] propose a multi-agent RL framework to train AVs in the presence of other vehicles, where different vehicle behavior is realized by adjusting the proportion between cooperative and selfish rewards. Hao *et al.* [12] use adversarial games and RL to test AV robustness to vehicles that are trained to cause AV failures (e.g., collisions) while exhibiting behaviors that mimic real-world driving action distributions (i.e., naturalistic priors). Wachi *et al.* [14] combine multi-agent games and adversarial RL [51] to discover failure cases for rule-based vehicles in simulation. Ma *et al.* [13] use level-k game theory [95] and RL to assess and improve an IDM decision-making mechanism (i.e., lane changing) in the presence of vehicles with manually defined reward functions that can exhibit cooperative or competitive behavior. However, game-based testing with RL approaches are often tightly coupled to specific types of vehicle models or a single dimension of human-based uncertainty and use ad-hoc development approaches for exploring different traffic scenarios. In contrast, our work provides a modular framework that uses goal models to declaratively specify human-based driving styles and supports the composition of these models to explore multiple dimensions of human-based uncertainty (i.e., different types and/or combinations of driving styles characterized by functional/non-functional objectives).

Other related work has explored testing AV behaviors in simulation. Dosovitskiy *et al.* [39], Son *et al.* [46], and Zhou *et al.* [47] proposed a number of simulation environments that can be used for AV testing. Birchler *et al.* [96], Zheng *et al.* [97], Zhong *et al.* [98] proposed several methods to generate test cases for an AV in simulation, but do not consider uncertainty from human-induced behaviors. Gambi *et al.* [48] combined procedural content generation and search-based testing to explore AV failure in various automatically generated traffic scenario settings. Humeniuk *et al.* [99] synthesized EC with RL to generate different scenarios to test autonomous systems, where RL is used to seed the EC search. Stocco *et al.* [100] introduced ThirdEye, a white-box AV failure predictor using machine learning that periodically monitors the AV’s reliability by identifying instances where the AV may be unconfident. While addressing robustness, they do not address human-induced uncertainty nor support a

1703 model-based approach. Fremont *et al.* [101] proposed Scenic, a probabilistic modeling
1704 language for specifying and generating a distribution of simulation environments for
1705 testing AVs. However, their approach focuses on modeling the environment and does
1706 not address means to capture non-functional objectives of agents in the environment.

1707 Other researchers have proposed model-based approaches for AVs or RL. Langford
1708 *et al.* [29] introduced MoDALAS, demonstrating a model-based approach to manage
1709 and verify the run-time assurance of machine learning components using KAOS goal
1710 models and utility functions. However, their approach does not consider human-based
1711 non-functional objectives when addressing run-time assurance. Liaskos *et al.* [102] pro-
1712 posed extending the i^* framework to model a formal specification for Markov decision
1713 processes. Rudolph *et al.* [103] proposed a method to identify and consider strategies
1714 of RL agents in the presence of other players for self-adaptation. Jiang *et al.* [104]
1715 proposed the THGC model, which uses prior domain knowledge to group agents in
1716 a multi-agent RL setting. Bruggner *et al.* [105] proposed a model-based approach to
1717 AV simulation, but models the different components of individual autonomous agents
1718 (i.e., perception, planning, and control). Leung *et al.* [106] introduced goal modeling
1719 for RL agents, where policies are represented as goals. However, their work does not
1720 use models to capture the high-level objectives of the agents and their interactions.
1721 Schwan *et al.* [55] proposed a goal specification language to formalize a reward func-
1722 tion for a given RL task (e.g., drive to destination). In contrast, our approach uses
1723 KAOS-inspired goal models to specify RL rewards as a means to train agents that
1724 exhibit specific driving styles, including those that are human-based.

1725 Finally, researchers have also proposed techniques that consider the role of
1726 humans during the development and deployment of cyber-physical systems (e.g.,
1727 AVs). Cleland-Huang *et al.* [107] and Camara *et al.* [108] focused on humans as
1728 an *internal* and *collaborative* contributor to provide decision-making support and
1729 other self-adaptive actions (e.g., MAPE-K actions [109]). Orthogonally, we focus on
1730 assessing/improving the robustness of AVs with respect to *external* human-based
1731 uncertainty in a *non-cooperative* setting. Gavidia-Calderon *et al.* [110] focused on the
1732 detection of different types of humans in the adaptive system’s environment, which
1733 then informs system adaptations. Our objective, in contrast, is to discover human-
1734 based uncertainty-induced *edge cases* that are detrimental to the safe operation of
1735 AVs.

1736

1737 7 Threats to Validity

1738

1739 This paper described an agent-based goal modeling approach to uncertainty discovery
1740 for AVs using non-cooperative game theory and RL. There may be possible deviations
1741 between agent behaviors observed in simulation and reality (i.e., “reality gap” [111]).
1742 Additionally, agents in simulation environments take synchronous actions, while real
1743 traffic interactions are asynchronous, which may contribute to the reality gap. The
1744 relevance of the discovered behavior is limited by how well the goal models capture
1745 the intended driving styles of vehicles in mixed-traffic interactions. The goal mod-
1746 els used in this work were designed by domain experts in the field of automotive
1747 assurance, and variations to the KAOS goal models may yield different experimental
1748

results [112]. Finally, repeated experiments may lead to or discover different types of agent behaviors or uncertainty, as RL uses stochastic processes to train agents. Additionally, RL algorithms may be sensitive to hyperparameter changes. In our studies, we used established defaults for the hyperparameters [16], with minor changes (e.g., number of training steps) to account for domain-specific/computational resource limits. To ensure the feasibility of the approach, each use case shows the result of an average of 100 episodes for comparison, similar to validation studies in other existing game-based testing approaches [12, 13].

8 Conclusion

This paper introduced the SAVVIDRIVER framework for using goal modeling to provide a systematic process in the RL-based realization of multi-agent game-based testing to discover unexpected behaviors. SAVVIDRIVER is a game-based testing framework that assesses the ability of the AV system to safely interact with various types of human drivers, who may exhibit a range of non-functional driving styles as they achieve their functional goals. Our framework promotes the discovery of interesting and/or unexpected behavior for both the EGO and the NEV(s), which can then be used to assess and improve the robustness of the AV with respect to multiple dimensions of human-based uncertainty.

We applied SAVVIDRIVER to three use cases to demonstrate the systematic refinement of high-level human driving styles and objectives into functional and non-functional goals, based on real-world traffic accident data [24, 67]. We implemented the multi-agent game-based testing using RL, based on the reusable goal models, and then demonstrated our framework’s ability to discover undesirable behavior in the AV under study. These failures are often caused by selfish, yet non-malicious objectives of the non-ego vehicles. We show that these use cases can discover failures in common challenging road scenes based on existing data from NHTSA and other traffic reports. For the ACC system use case, we were able to use SAVVIDRIVER to discover undesirable behaviors, where the failure traces led to a similar set of changes recommended by the OEM during the early deployment stages of the ACC systems [90, 91]

Several directions are being considered for future work. For example, we will explore the training of multiple RL agents with additional driving styles (e.g., timid, intoxicated, etc.) and their composition(s) within a given agent to discover unique strategies of agents and potentially reduce training time. Additional studies may explore how evolutionary computation can be used to explore different gradients and/or combinations of human driving styles (i.e., different levels of aggressiveness or speeding). Other research may investigate the use of procedural content generation to automatically create traffic scenarios for study, including those with various environmental conditions (e.g., slippery road surfaces, road obstacles, potholes, etc.), city-scale traffic environments, and large-scale intelligent transportation systems.

Acknowledgments

We greatly appreciate contributions from Nick Polanco on our preliminary work. We also thank Joshua E. Siegel and Shaunak D. Bopardikar for the insightful discussions

1795 and detailed feedback on our framework. This work was supported in part by funding
1796 provided by Michigan State University. Finally, we gratefully acknowledge the detailed
1797 feedback provided by the reviewers on earlier versions of this paper.

1798

1799 References

1800

- 1801 [1] Chen, B., Sun, D., Zhou, J., Wong, W. & Ding, Z. A future intelligent traffic
1802 system with mixed autonomous vehicles and human-driven vehicles. *Information*
1803 *Sciences* **529**, 59–72 (2020).
- 1804 [2] Rushby, J. Logic and Epistemology in Safety Cases. *Lecture Notes in Computer*
1805 *Science* 1–7 (2013).
- 1806 [3] Hüllermeier, E. & Waegeman, W. Aleatoric and epistemic uncertainty in
1807 machine learning: An introduction to concepts and methods. *Machine Learning*
1808 **110**, 457–506 (2021).
- 1809 [4] Ramirez, A. J., Jensen, A. C. & Cheng, B.H.C.. *A taxonomy of uncertainty for*
1810 *dynamically adaptive systems*. *2012 7th International Symposium on Software*
1811 *Engineering for Adaptive and Self-Managing Systems (SEAMS)*, 99–108 (IEEE,
1812 Zurich, Switzerland, 2012).
- 1813 [5] Wachenfeld, W. & Winner, H. The release of autonomous vehicles. *Autonomous*
1814 *Driving: Technical, Legal and Social Aspects* 425–449 (2016).
- 1815 [6] Haq, F. U., Shin, D., Nejati, S. & Briand, L. Can Offline Testing of Deep Neural
1816 Networks Replace Their Online Testing? *Empirical Software Engineering* **26**,
1817 90 (2021).
- 1818 [7] Chan, K. H., Zilberman, S., Polanco, N., Siegel, J. E. & Cheng, B.H.C..
1819 *SafeDriveRL: Combining Non-cooperative Game Theory with Reinforcement*
1820 *Learning to Explore and Mitigate Human-based Uncertainty for Autonomous*
1821 *Vehicles*. *Proceedings of the 19th International Conference on Adaptive and*
1822 *Self-Managing Systems (SEAMS 2024)*, 214–220 (2024). Short Paper.
- 1823 [8] Yang, K. *et al.* Uncertainties in onboard algorithms for autonomous vehicles:
1824 Challenges, mitigation, and perspectives. *IEEE Transactions on Intelligent*
1825 *Transportation Systems* **24**, 8963–8987 (2023).
- 1826 [9] Burton, S. & Herd, B. Addressing uncertainty in the safety assurance of machine-
1827 learning. *Frontiers in Computer Science* **5**, 1132580 (2023).
- 1828 [10] Chao, Q. *et al.* A survey on visual traffic simulation: Models, evaluations, and
1829 applications in autonomous driving **39**, 287–308 (2020).
- 1830 [11] Nash, J. Non-cooperative games. *Annals of Mathematics* **54**, 286–295 (1951).
1831 URL <http://www.jstor.org/stable/1969529>.
- 1832 [12] Hao, K. *et al.* Adversarial Safety-Critical Scenario Generation using Naturalistic
1833 Human Driving Priors. *IEEE Transactions on Intelligent Vehicles* 1–16 (2023).
- 1834 [13] Ma, Y. *et al.* Evolving testing scenario generation and intelligence evaluation
1835 for automated vehicles. *Transportation Research Part C: Emerging Technologies*
1836 **163**, 104620 (2024).
- 1837 [14] Wachi, A. Failure-scenario maker for rule-based agent using multi-agent adver-
1838 sarial reinforcement learning and its application to autonomous driving (2019).
- 1839 [15] Liu, W. *et al.* Learning to model diverse driving behaviors in highly interactive
1840

autonomous driving scenarios with multiagent reinforcement learning. <i>IEEE Systems Journal</i> (2025).	1841 1842
[16] Schulman, J., Wolski, F., Dhariwal, P., Radford, A. & Klimov, O. Proximal Policy Optimization Algorithms (2017). arxiv:arXiv:1707.06347 .	1843 1844
[17] Cao, Z. <i>et al.</i> Reinforcement learning based control of imitative policies for near-accident driving. <i>Robotics: Science and Systems</i> (2020).	1845 1846
[18] Gupta, P., Coleman, D. & Siegel, J. E. Towards physically adversarial intelligent networks (pains) for safer self-driving. <i>IEEE Control Systems Letters</i> 7 , 1063–1068 (2022).	1847 1848 1849
[19] Folkers, A., Rick, M. & Büskens, C. Controlling an Autonomous Vehicle with Deep Reinforcement Learning. <i>2019 IEEE Intelligent Vehicles Symposium (IV)</i> , 2025–2031 (2019). arxiv:1909.12153 .	1850 1851 1852
[20] IEEE. A review of reward functions for reinforcement learning in the context of autonomous driving.	1853 1854
[21] Ramirez, A. J., Jensen, A. C., Cheng, B.H.C.. & Knoester, D. B. Automatically exploring how uncertainty impacts goal satisfaction. <i>Proceedings of International Conference on Automated Software Engineering (ASE 2011)</i> , 568–571 (2011).	1855 1856 1857
[22] Dijkstra, E. W. On the role of scientific thought. <i>Selected writings on computing: a personal perspective</i> 60–66 (1982).	1858 1859
[23] Parnas, D. L. On the criteria to be used in decomposing systems into modules. <i>Communications of the ACM</i> 15 , 1053–1058 (1972).	1860 1861
[24] Media, NHTSA. Driving behaviors reported for drivers and motorcycle operators involved in fatal crashes. https://www.iii.org/fact-statistic/facts-statistics-aggressive-driving (2021).	1862 1863 1864
[25] Media, NHTSA. Nhtsa estimates for 2022 show roadway fatalities remain flat after two years of dramatic increases. https://www.nhtsa.gov/press-releases/traffic-crash-death-estimates-2022 (2023).	1865 1866 1867
[26] Richard, C. M., Campbell, J. L., Brown, J. L. <i>et al.</i> Task analysis of intersection driving scenarios: Information processing bottlenecks. Tech. Rep., Turner-Fairbank Highway Research Center (2006).	1868 1869 1870
[27] van Lamsweerde, A. <i>Goal-oriented requirements engineering: A guided tour</i> . <i>Proceedings Fifth IEEE International Symposium on Requirements Engineering</i> , 249–262 (2001).	1871 1872 1873
[28] Walsh, W. E., Tesauro, G., Kephart, J. O. & Das, R. Utility functions in autonomic systems. <i>International Conference on Autonomic Computing, 2004. Proceedings.</i> , 70–77 (IEEE, 2004).	1874 1875 1876
[29] Langford, M. A., Chan, K. H., Fleck, J. E., McKinley, P. K. & Cheng, B.H.C.. <i>Modalas: Model-driven assurance for learning-enabled autonomous systems</i> . <i>2021 ACM/IEEE 24th International Conference on Model Driven Engineering Languages and Systems (MODELS)</i> , 182–193 (IEEE, 2021).	1877 1878 1879 1880
[30] Thwarted on the On-ramp: Waymo Driverless Car Doesn't Feel the Urge to Merge. https://www.thetruthaboutcars.com/2018/05/thwarted-ramp-waymo-driverless-car-doesnt-feel-urge-merge/ (2018).	1881 1882 1883
[31] Bradley, R. Tesla Autopilot. https://www.technologyreview.com/technology/tesla-autopilot/ .	1884 1885 1886

- 1887 [32] Freedman, I. G., Kim, E. & Muennig, P. A. Autonomous vehicles are cost-
1888 effective when used as taxis. *Injury epidemiology* **5**, 1–8 (2018).
- 1889 [33] Us, Y. Overcoming deployment hurdles: Adastec’s approach to auto-
1890 mated bus integration (2023). URL <https://www.adastec.com/post/overcoming-deployment-hurdles>.
- 1892 [34] Team, T. W. Waymo significantly outperforms comparable
1893 human benchmarks over 7+ million miles of rider-only driving.
1894 <https://waymo.com/blog/2023/12/waymo-significantly-outperforms-comparable-human-benchmarks-over-7-million>.
- 1896 [35] Koopman, P., Osyk, B. & Weast, J. *Autonomous vehicles meet the physical
1897 world: Rss, variability, uncertainty, and proving safety. Computer Safety, Reli-
1898 ability, and Security: 38th International Conference, SAFECOMP 2019, Turku,
1899 Finland, September 11–13, 2019, Proceedings* **38**, 245–253 (Springer, 2019).
- 1900 [36] Sagberg, F., Selpi, Bianchi Piccinini, G. F. & Engström, J. A review of research
1901 on driving styles and road safety. *Human factors* **57**, 1248–1275 (2015).
- 1902 [37] Paleti, R., Eluru, N. & Bhat, C. R. Examining the influence of aggressive driv-
1903 ing behavior on driver injury severity in traffic crashes. *Accident Analysis &
1904 Prevention* **42**, 1839–1854 (2010).
- 1905 [38] Antić, B., Čabarkapa, M., Čubranić-Dobrodolac, M. & Čičević, S. The influ-
1906 ence of aggressive driving behavior and impulsiveness on traffic accidents. *US
1907 Transportation Collection* (2018).
- 1908 [39] Dosovitskiy, A., Ros, G., Codevilla, F., Lopez, A. & Koltun, V. *Carla: An open
1909 urban driving simulator. Conference on robot learning*, 1–16 (PMLR, 2017).
- 1910 [40] BeamNG GmbH. BeamNG.tech. URL <https://www.beamng.tech/>.
- 1911 [41] Bernhard, J., Esterle, K., Hart, P. & Kessler, T. *Bark: Open behavior benchmark-
1912 ing in multi-agent environments. 2020 IEEE/RSJ International Conference on
1913 Intelligent Robots and Systems (IROS)* (2020). URL <https://arxiv.org/pdf/2003.02604.pdf>.
- 1915 [42] Leurent, E. An environment for autonomous driving decision-making. <https://github.com/eleurent/highway-env> (2018).
- 1917 [43] Menon, C. & Alexander, R. A safety-case approach to the ethics of autonomous
1918 vehicles. *Safety and reliability* **39**, 33–58 (2020).
- 1919 [44] Chowdhury, T., Wassnyg, A., Paige, R. F. & Lawford, M. *Systematic evalua-
1920 tion of (safety) assurance cases. International Conference on Computer Safety,
1921 Reliability, and Security*, 18–33 (Springer, 2020).
- 1922 [45] Mohamad, M., Åström, A., Askerdal, Ö., Borg, J. & Scandariato, R. *Secu-
1923 rity assurance cases for road vehicles: An industry perspective. Proceedings of
1924 the 15th International Conference on Availability, Reliability and Security*, 1–6
1925 (2020).
- 1926 [46] Son, T. D., Bhave, A. & Van der Auweraer, H. *Simulation-based testing frame-
1927 work for autonomous driving development. 2019 IEEE International Conference
1928 on Mechatronics (ICM)*, Vol. 1, 576–583 (IEEE, 2019).
- 1929 [47] Zhou, L. et al. *Garchingsim: An autonomous driving simulator with photoreal-
1930 istic scenes and minimalist workflow. 2023 IEEE 26th International Conference
1931 on Intelligent Transportation Systems (ITSC)*, 4227–4232 (IEEE, 2023).

- [48] Gambi, A., Mueller, M. & Fraser, G. *Automatically testing self-driving cars with search-based procedural content generation*. *Proceedings of the 28th ACM SIGSOFT International Symposium on Software Testing and Analysis*, 318–328 (2019).
- [49] Leventhal, L. M., Teasley, B. M., Rohlman, D. S. & Instone, K. *Positive test bias in software testing among professionals: A review*. *Human-Computer Interaction: Third International Conference, EWHCI'93 Moscow, Russia, August 3–7, 1993 Selected Papers 3*, 210–218 (Springer, 1993).
- [50] Rapoport, A. *Game theory as a theory of conflict resolution* Vol. 2 (Springer Science & Business Media, 2012).
- [51] Pinto, L., Davidson, J., Sukthankar, R. & Gupta, A. *Robust adversarial reinforcement learning*. *International conference on machine learning*, 2817–2826 (PMLR, 2017).
- [52] Liniger, A. & Lygeros, J. A noncooperative game approach to autonomous racing. *IEEE Transactions on Control Systems Technology* **28**, 884–897 (2019).
- [53] Arulkumaran, K., Deisenroth, M. P., Brundage, M. & Bharath, A. A. Deep reinforcement learning: A brief survey. *IEEE Signal Processing Magazine* **34**, 26–38 (2017).
- [54] Kiran, B. R. *et al.* Deep reinforcement learning for autonomous driving: A survey. *IEEE transactions on intelligent transportation systems* **23**, 4909–4926 (2021).
- [55] Schwan, S., Klös, V. & Glesner, S. *A goal-oriented specification language for reinforcement learning*. *International Conference on Modeling Decisions for Artificial Intelligence*, 169–180 (Springer, 2023).
- [56] Kaelbling, L. P., Littman, M. L. & Moore, A. W. Reinforcement learning: A survey. *Journal of artificial intelligence research* **4**, 237–285 (1996).
- [57] Tzorakoleftherakis, E. Reinforcement Learning: A Brief Guide. <https://www.mathworks.com/company/technical-articles/reinforcement-learning-a-brief-guide.html> (2019).
- [58] Konda, V. & Tsitsiklis, J. Actor-critic algorithms. *Advances in neural information processing systems* **12** (1999).
- [59] Elsayed, M., Lan, Q., Lyle, C. & Mahmood, A. R. Weight clipping for deep continual and reinforcement learning. *arXiv preprint arXiv:2407.01704* (2024).
- [60] Williams, R. J. Simple statistical gradient-following algorithms for connectionist reinforcement learning. *Machine learning* **8**, 229–256 (1992).
- [61] Mnih, V. *et al.* Asynchronous methods for deep reinforcement learning. *International conference on machine learning*, 1928–1937 (PMLR, 2016).
- [62] Sutton, R. S., Barto, A. G. *et al.* Reinforcement learning. *Journal of Cognitive Neuroscience* **11**, 126–134 (1999).
- [63] Garlan, D., Cheng, S.-W., Huang, A.-C., Schmerl, B. & Steenkiste, P. Rainbow: Architecture-based self-adaptation with reusable infrastructure. *Computer* **37**, 46–54 (2004).
- [64] Ramirez, A. J. & Cheng, B.H.C.. Automatic derivation of utility functions for monitoring software requirements. *International Conference on Model Driven Engineering Languages and Systems*, 501–516 (Springer, 2011).

- 1979 [65] DeGrandis, P. & Valetto, G. *Elicitation and utilization of application-level util-*
 1980 *ity functions. Proceedings of the 6th international conference on Autonomic*
 1981 *computing*, 107–116 (2009).
- 1982 [66] Fredericks, E. M. *Automatically hardening a self-adaptive system against uncer-*
 1983 *tainty. Proceedings of the 11th International Symposium on Software Engineer-*
 1984 *ing for Adaptive and Self-Managing Systems, SEAMs '16*, 16–27 (Association
 1985 for Computing Machinery, New York, NY, USA, 2016). URL <http://doi.org/10.1145/2897053.2897059>.
- 1987 [67] Media, NHTSA. Distracted driving. <https://www.nhtsa.gov/risky-driving/distracted-driving> (2021).
- 1989 [68] Gross, A. Risky business – more than half of all drivers engage in dangerous
 1990 behavior. <https://newsroom.aaa.com/2023/11/risky-business-more-than-half-of-all-drivers-engage-in-dangerous-behavior/> (2023).
- 1992 [69] Media, A. Likelihood of aggressive driving among u.s. drivers (2019). URL
 1993 <https://exchange.aaa.com/safety/driving-advice/aggressive-driving/>.
- 1994 [70] Mergia, W. Y., Eustace, D., Chimba, D. & Qumsiyeh, M. Exploring factors
 1995 contributing to injury severity at freeway merging and diverging locations in
 1996 ohio. *Accident Analysis & Prevention* **55**, 202–210 (2013).
- 1997 [71] Luo, Y. et al. *A Driving Intention Prediction Method for Mixed Traffic Sce-*
 1998 *narios. 2022 IEEE 7th International Conference on Intelligent Transportation*
 1999 *Engineering (ICITE)*, 296–301 (IEEE, Beijing, China, 2022).
- 2000 [72] Fujiwara-Greve, T. in *Nash Equilibrium* (ed. Fujiwara-Greve, T.) *Non-*
 2001 *Cooperative Game Theory* Monographs in Mathematical Economics, 23–55
 2002 (Springer Japan, Tokyo, 2015).
- 2003 [73] Fudenberg, D. & Tirole, J. Noncooperative game theory for industrial organiza-
 2004 tion: an introduction and overview. *Handbook of industrial Organization* **1**,
 2005 259–327 (1989).
- 2006 [74] Lanctot, M. et al. *A unified game-theoretic approach to multiagent reinforcement*
 2007 *learning. Advances in Neural Information Processing Systems*, Vol. 30 (Curran
 2008 Associates, Inc., 2017). URL https://proceedings.neurips.cc/paper_files/paper/2017/file/3323fe11e9595c09af38fe67567a9394-Paper.pdf.
- 2010 [75] Huck, T. P., Ledermann, C. & Kröger, T. *Simulation-based testing for early*
 2011 *safety-validation of robot systems. 2020 IEEE Symposium on Product Compli-*
 2012 *ance Engineering-(SPCE Portland)*, 1–6 (IEEE, 2020).
- 2013 [76] Koopman, P. & Wagner, M. Toward a framework for highly automated vehicle
 2014 safety validation. Tech. Rep., SAE Technical Paper (2018).
- 2015 [77] Abbas, H., O'Kelly, M., Rodionova, A. & Mangharam, R. *Safe at any speed: A*
 2016 *simulation-based test harness for autonomous vehicles. Cyber Physical Systems.*
 2017 *Design, Modeling, and Evaluation: 7th International Workshop, CyPhy 2017,*
 2018 *Seoul, South Korea, October 15-20, 2017, Revised Selected Papers* **7**, 94–106
 2019 (Springer, 2019).
- 2020 [78] Treiber, M., Hennecke, A. & Helbing, D. Congested traffic states in empirical
 2021 observations and microscopic simulations. *Physical review E* **62**, 1805 (2000).
- 2022 [79] Types of Unsignalized Intersections - Unsignalized Intersection Improvement
 2023 Guide. <https://toolkits.ite.org/uiig/types.aspx>.
- 2024

- [80] National Highway Traffic Safety Administration. Query of fatality analysis reporting system (fars) web-based encyclopedia. <https://www.safercar.gov/research-data/fatality-analysis-reporting-system-fars> (2014). Accessed: 2014-12-04. 2025
2026
2027
2028
- [81] Liberatore, S. Self-driving race car crashes into a wall from the starting line. <https://www.dailymail.co.uk/sciencetech/article-8899021/Self-driving-race-car-crashes-straight-wall-starting-line-Roborace.html> (2020). 2029
2030
2031
- [82] Kong, J., Pfeiffer, M., Schildbach, G. & Borrelli, F. *Kinematic and dynamic vehicle models for autonomous driving control design*. 2015 IEEE intelligent vehicles symposium (IV), 1094–1099 (IEEE, 2015). 2032
2033
2034
- [83] Koenig, N. & Howard, A. *Design and use paradigms for gazebo, an open-source multi-robot simulator*. 2004 IEEE/RSJ International Conference on Intelligent Robots and Systems (IROS)(IEEE Cat. No. 04CH37566), Vol. 3, 2149–2154 (IEEE, 2004). 2035
2036
2037
2038
- [84] Brockman, G. *et al.* Openai gym. *arXiv preprint arXiv:1606.01540* (2016). 2039
- [85] Westhofen, L. *et al.* Criticality Metrics for Automated Driving: A Review and Suitability Analysis of the State of the Art. *Archives of Computational Methods in Engineering* **30**, 1–35 (2023). 2040
2041
2042
- [86] Minderhoud, M. M. & Bovy, P. H. Extended time-to-collision measures for road traffic safety assessment. *Accident Analysis & Prevention* **33**, 89–97 (2001). 2043
2044
- [87] Saffarzadeh, M., Nadimi, N., Naseralavi, S. & Mamdoohi, A. R. *A general formulation for time-to-collision safety indicator*. Proceedings of the Institution of Civil Engineers-Transport, Vol. 166, 294–304 (Thomas Telford Ltd, 2013). 2045
2046
2047
- [88] Choi, E.-H. Crash Factors in Intersection-Related Crashes: An On-Scene Perspective: (621942011-001) (2010). 2048
2049
- [89] Langford, M. A., Zilberman, S. & Cheng, B.H.C.. Anunnaki: A modular framework for developing trusted artificial intelligence. *ACM Trans. Auton. Adapt. Syst.* (2024). URL <https://doi-org.proxy2.cl.msu.edu/10.1145/3649453>. 2050
2051
2052
- [90] Barry, K. Guide to Adaptive Cruise Control. <https://www.consumerreports.org/cars/car-safety/guide-to-adaptive-cruise-control-a9154580873/> (2022). 2053
2054
2055
- [91] Company, F. M. Adaptive cruise control - setting the adaptive cruise control gap (2021). URL https://www.fordservicecontent.com/Ford_Content/vdirsnet/OwnerManual/Home/Content?variantid=7505&languageCode=en&countryCode=USA&Uid=G2047539&ProcUid=G2045342&userMarket=USA&div=f&vFilteringEnabled=False&buildtype=web. 2056
2057
2058
2059
2060
- [92] Langford, M. A. & Cheng, B.H.C.. Enki: A Diversity-driven Approach to Test and Train Robust Learning-enabled Systems. *ACM Transactions on Autonomous and Adaptive Systems* **15**, 1–32 (2020). 2061
2062
2063
- [93] Li, N. *et al.* Game theoretic modeling of driver and vehicle interactions for verification and validation of autonomous vehicle control systems. *IEEE Transactions on control systems technology* **26**, 1782–1797 (2017). 2064
2065
2066
- [94] Zhou, W., Cao, Z., Deng, N., Jiang, K. & Yang, D. Identify, estimate and bound the uncertainty of reinforcement learning for autonomous driving. *IEEE Transactions on Intelligent Transportation Systems* **24**, 7932–7942 (2023). 2067
2068
2069
2070

- 2071 [95] Peters, H. *Game theory: A Multi-leveled approach* (Springer, 2015).
- 2072 [96] Birchler, C., Khatiri, S., Bosshard, B., Gambi, A. & Panichella, S. Machine
2073 learning-based test selection for simulation-based testing of self-driving cars
2074 software. *Empirical Software Engineering* **28**, 71 (2023).
- 2075 [97] Zheng, X. *et al.* Rapid generation of challenging simulation scenarios for
2076 autonomous vehicles based on adversarial test. *2020 IEEE International Con-*
2077 *ference on Mechatronics and Automation (ICMA)*, 1166–1172 (IEEE, 2020).
- 2078 [98] Zhong, Z., Kaiser, G. & Ray, B. Neural network guided evolutionary fuzzing for
2079 finding traffic violations of autonomous vehicles. *IEEE Transactions on Software
2080 Engineering* (2022).
- 2081 [99] Humeniuk, D., Khomh, F. & Antoniol, G. Reinforcement learning informed
2082 evolutionary search for autonomous systems testing. *ACM Transactions on
2083 Software Engineering and Methodology* **33**, 1–45 (2024).
- 2084 [100] Stocco, A., Nunes, P. J., d’Amorim, M. & Tonella, P. *Thirdeye: Attention
2085 maps for safe autonomous driving systems*. *Proceedings of the 37th IEEE/ACM
2086 International Conference on Automated Software Engineering*, 1–12 (2022).
- 2087 [101] Fremont, D. J. *et al.* Scenic: A language for scenario specification and data
2088 generation. *Machine Learning* **112**, 3805–3849 (2023).
- 2089 [102] Liaskos, S., Khan, S. M., Golipour, R. & Mylopoulos, J. *Towards goal-based
2090 generation of reinforcement learning domain simulations*. *iStar*, 22–28 (2022).
- 2091 [103] Rudolph, S., Tomforde, S. & Hähner, J. On the detection of mutual influ-
2092 ences and their consideration in reinforcement learning processes. *arXiv preprint
2093 arXiv:1905.04205* (2019).
- 2094 [104] Jiang, H. *et al.* Multi-agent deep reinforcement learning with type-based
2095 hierarchical group communication. *Applied Intelligence* **51**, 5793–5808 (2021).
- 2096 [105] Bruggner, D., Hegde, A., Acerbo, F. S., Gulati, D. & Son, T. D. *Model in the
2097 loop testing and validation of embedded autonomous driving algorithms*. *2021
2098 IEEE Intelligent Vehicles Symposium (IV)*, 136–141 (IEEE, 2021).
- 2099 [106] Leung, J., Shen, Z., Zeng, Z. & Miao, C. *Goal modelling for deep reinforce-
2100 ment learning agents*. *Machine Learning and Knowledge Discovery in Databases.
2101 Research Track: European Conference, ECML PKDD 2021, Bilbao, Spain,
2102 September 13–17, 2021, Proceedings, Part I* **21**, 271–286 (Springer, 2021).
- 2103 [107] Cleland-Huang, J. *et al.* Human–machine Teaming with Small Unmanned Aerial
2104 Systems in a MAPE-K Environment. *ACM Transactions on Autonomous and
2105 Adaptive Systems* **19**, 1–35 (2024).
- 2106 [108] Cámará, J., Moreno, G. & Garlan, D. Reasoning about Human Participation
2107 in Self-Adaptive Systems. *2015 IEEE/ACM 10th International Symposium on
2108 Software Engineering for Adaptive and Self-Managing Systems* 146–156 (2015).
- 2109 [109] Arcaini, P., Riccobene, E. & Scandurra, P. *Modeling and analyzing MAPE-K
2110 feedback loops for self-adaptation*. *2015 IEEE/ACM 10th International Sympo-
2111 sium on Software Engineering for Adaptive and Self-Managing Systems*, 13–23
2112 (IEEE, 2015).
- 2113 [110] Gavidia-Calderon, C., Kordon, A., Bennaceur, A., Levine, M. & Nuseibeh, B.
2114 The IDEA of Us: An Identity-Aware Architecture for Autonomous Systems.
2115 *ACM Transactions on Software Engineering and Methodology* **33**, 1–38 (2024).
- 2116

- [111] Combemale, B. *et al.* A Hitchhiker’s Guide to Model-Driven Engineering for Data-Centric Systems. *IEEE Software* **38**, 71–84 (2021). 2117
2118
- [112] Franch, X. The i* framework: The way ahead. *2012 Sixth International Conference on Research Challenges in Information Science (RCIS)* 1–3 (2012). 2119
2120
2121
2122
2123
2124
2125
2126
2127
2128
2129
2130
2131
2132
2133
2134
2135
2136
2137
2138
2139
2140
2141
2142
2143
2144
2145
2146
2147
2148
2149
2150
2151
2152
2153
2154
2155
2156
2157
2158
2159
2160
2161
2162